



Making the Most of Offshore Wind

Re-Evaluating the Potential of Offshore Wind in the German North Sea

STUDY



PUBLICATION DETAILS

Making the Most of Offshore Wind

Re-Evaluating the Potential of Offshore Wind in the German North Sea

COMMISSIONED BY

Agora Energiewende
www.agora-energiewende.de
info@agora-energiewende.de

Agora Verkehrswende
www.agora-verkehrswende.de
info@agora-verkehrswende.de

Anna-Louisa-Karsch-Straße 2 | 10178 Berlin
T +49 (0)30 700 14 35-000
F +49 (0)30 700 14 35-129

PROJECT MANAGEMENT

Matthias Deutsch, Agora Energiewende
matthias.deutsch@agora-energiewende.de

STUDY BY

Technical University of Denmark,
Department of Wind Energy
DTU Wind Energy | DTU Campus Risø
Frederiksborgvej 399 | DK- 4000 Roskilde
Jake Badger, Marc Imberger, Patrick Volker (formerly
DTU Wind Energy)

Max-Planck-Institute for Biogeochemistry,
Biospheric Theory and Modeling
Hans-Knöll-Str. 10 | 07745 Jena
Axel Kleidon, Sonja Germer (formerly MPI-BGC),
Jonathan Minz

Typesetting: Ada Rühring
Proofreading: WordSolid
Cover: Nicholas Free, iStockphoto

176/01-S-2020/EN

36-2020-EN

Version: 1.1, March 2020

ACKNOWLEDGEMENTS

We would like to thank Andreas Graf, Thorsten Lenck, Frank Peter, Christoph Podewils and Georg Thomassen (all Agora Energiewende) for their helpful comments. We would also like to thank all those who participated in the expert workshops for their valuable input.

The Technical University of Denmark and the Max-Planck-Institute for Biogeochemistry are solely responsible for the findings of this study. The conclusions reflect the opinions of Agora Energiewende and Agora Verkehrswende.



This publication is available for
download under this QR code.

Please cite as:

Agora Energiewende, Agora Verkehrswende, Technical University of Denmark and Max-Planck-Institute for Biogeochemistry (2020): Making the Most of Offshore Wind: Re-Evaluating the Potential of Offshore Wind in the German North Sea.

Conclusions and the main section should be cited as indicated on page 7 and 29, respectively.

www.agora-energiewende.de

Preface

Dear reader,

as part of its European Green Deal, the European Commission has announced to present a strategy on offshore wind in 2020. Such a strategy is urgently needed as reaching a climate-neutral Europe will require a massive expansion of offshore wind energy.

This raises the question whether energy models used today by wind farm planners and investors can adequately capture the interaction effects between turbines stemming from very large areas covered with offshore wind farms at high installed capacity density. To better understand such effects, Agora Energiewende and Agora Verkehrswende commissioned the Department of Wind Energy at the Technical University of Denmark as well as the Max-Planck-Institute for Biogeochemistry to simulate future offshore wind expansion scenarios

for the German section of the North Sea with two distinct modelling approaches. This study presents the findings, and it underscores the importance of the role of the state in planning for a future with a lot more offshore wind energy.

We hope you find the study to be an inspiring and enjoyable read!

Yours sincerely,

Patrick Graichen

Executive Director of Agora Energiewende

Christian Hochfeld

Executive Director of Agora Verkehrswende

Key conclusions:

1

Offshore wind energy, which has an installed capacity potential of up to 1,000 GW, is a key pillar of the European energy transition. The net-zero decarbonization scenarios contained in the European Commission's Long-Term Strategy assume some 400 to 450 GW of offshore wind capacity by 2050. Additional demand of up to 500 GW may be created by dedicating offshore farms to electrolysis for renewable hydrogen production.

2

Scenarios projecting near climate neutrality by 2050 assume an installed capacity of 50 to 70 GW of offshore wind in Germany, generating some 200 to 280 TWh of electricity per year. Given the 6 GW of installed capacity today and current plans for 20 GW by 2030, the pace of spatial planning for offshore wind deployment needs to pick up significantly. The slowing of onshore wind development could further enhance the importance of offshore wind in achieving net zero.

3

Offshore wind power needs sufficient space, as the full load operating time may otherwise shrink from currently around 4,000 hours per year to between 3,000 and 3,300 hours. The more turbines are installed in a region, the less efficient offshore wind production becomes due to a lack of wind recovery. If Germany were to install 50 to 70 GW solely in the German Bight, the number of full-load hours achieved by offshore wind farms would decrease considerably.

4

Countries on the North and Baltic Seas should cooperate with a view to maximizing the wind yield and full-load hours of their offshore wind farms. In order to maximize the efficiency and potential of offshore wind, the planning and development of wind farms – as well as broader maritime spatial planning – should be intelligently coordinated across national borders. This finding is relevant to both the North and Baltic Seas. In addition, floating offshore wind farms could enable the creative integration of deep waters into wind farm planning.

Content

Making the Most of Offshore Wind: Re-Evaluating the Potential of Offshore Wind in the German North Sea

Conclusions drawn by Agora Energiewende and Agora Verkehrswende

| | | |
|---|-------------|----|
| 1 | Conclusions | 9 |
| 2 | References | 23 |

Making the Most of Offshore Wind: Re-Evaluating the Potential of Offshore Wind in the German North Sea

Technical University of Denmark and Max-Planck-Institute

| | | |
|---|---|----|
| 1 | Summary | 31 |
| 2 | Background: More than wakes | 35 |
| 3 | Goals and offshore wind expansion scenarios | 39 |
| | 3.1 Suitable areas for offshore wind energy | 40 |
| | 3.2 Assumed turbine technology | 41 |
| | 3.3 Definition of scenarios | 41 |
| | 3.4 Typical wind climatology in the region | 42 |
| 4 | Methods | 43 |
| | 4.1 Overview | 43 |
| | 4.2 KEBA: Kinetic Energy Budget of the Atmosphere | 44 |
| | 4.3 WRF: Weather Research and Forecasting Model | 45 |
| 5 | Results | 51 |
| | 5.1 Overview | 51 |
| | 5.2 KEBA results | 51 |
| | 5.3 WRF results | 55 |
| | 5.4 Comparison and interpretation | 61 |
| 6 | Conclusions | 67 |
| 7 | Recommendations | 69 |
| 8 | References | 71 |
| 9 | Appendices | 73 |
| | 9.1 Parameter values used for the KEBA method | 73 |
| | 9.2 Cross-sectional widths and downwind lengths used in the KEBA “directions” estimates | 73 |
| | 9.3 Namelist for the WRF mesoscale model | 77 |

Making the Most of Offshore Wind: Re-Evaluating the Potential of Offshore Wind in the German North Sea

Conclusions drawn by
Agora Energiewende and
Agora Verkehrswende

Please cite as:

Agora Energiewende and Agora Verkehrswende (2020):
Making the Most of Offshore Wind: Re-Evaluating
the Potential of Offshore Wind in the German North
Sea. Conclusions drawn by Agora Energiewende and
Agora Verkehrswende. In: Agora Energiewende, Agora
Verkehrswende, Technical University of Denmark and
Max-Planck-Institute for Biogeochemistry (2020):
Making the Most of Offshore Wind: Re-Evaluating the
Potential of Offshore Wind in the German North Sea.

Conclusions

1

Offshore wind energy, which has an installed capacity potential of up to 1,000 GW, is a key pillar of the European energy transition.

Achieving the goals of the Paris Agreement will require Europe to move ever closer to a climate-neutral energy system.¹ In this transition toward very high shares of variable renewable energy sources like solar PV and wind, offshore wind will play a crucial role.

Offshore wind comes with desirable properties that onshore wind and solar PV cannot offer: high full-load hours, high operating hours, rather low variability and – consequently – greater predictability than

onshore wind, including correspondingly lower forecast errors and balancing power requirements.² Due to these features, offshore wind's system value is generally higher than that of onshore wind and more stable over time than that of solar PV.³ Regarding system adequacy, offshore wind can contribute around 30% of its installed capacity to the ability of the power system to match generation with consumption at all times, thereby reducing the need for investment into dispatchable backup power plants. In

1 EC (2018a)

2 Stiftung Offshore (2017)

3 IEA (2019)

Achievable full-load hours for very good sites assumed in modelling commissioned by the European Commission

Figure 1



Note: Each band indicates an estimated range. Figures extend from 2020 to 2050.

ASSET (2018)

the future, offshore wind could also provide flexibility services.⁴

Whereas solar PV and onshore wind power generation are assumed to reach up to 2,300 and 3,700 full-load hours at very good sites, offshore wind is believed to reach up to 5,200 full-load hours (i.e. a capacity factor of 59%), as illustrated in Figure 1.⁵

While the levelized cost of electricity (LCOE) generated by offshore wind declined from about 0.15 USD/kWh to 0.13 USD/kWh between 2010 and 2018⁶, strike prices in recent auctions in Europe have fallen to almost 0.05 USD/kWh for delivery in the mid-2020s, and the confidence of investors into

offshore wind is growing, thereby reducing financing costs. New technological developments such as floating foundations may further advance the deployment of offshore wind energy in parts of Europe and abroad.⁷

The net-zero decarbonization scenarios contained in the European Commission’s Long-Term Strategy assume some 400 to 450 GW of offshore wind capacity by 2050.

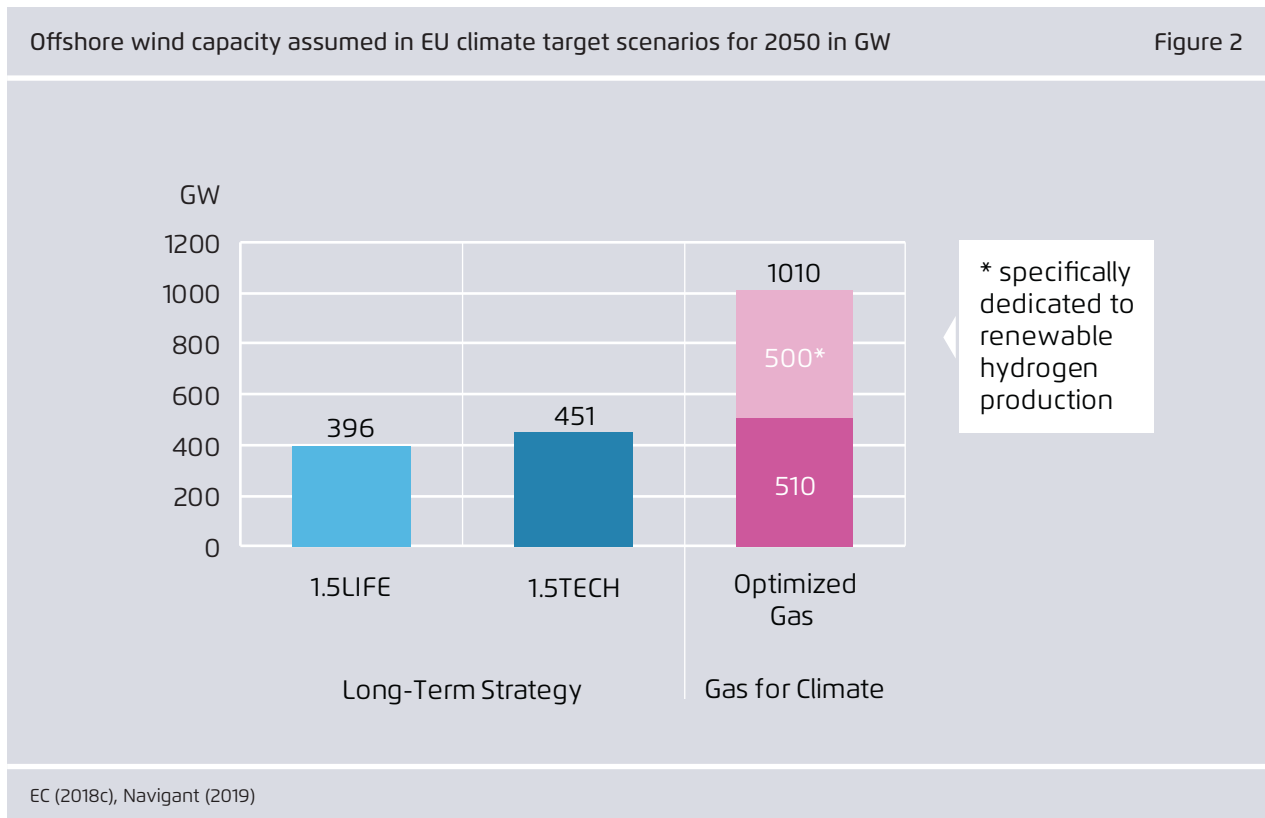
With its Long-Term Strategy, the European Commission has explored several pathways to reduce greenhouse gas emissions, from scenarios that address the well below 2°C target to those that pursue efforts to limit temperature change to 1.5°C. The latter goal is forecast in the 1.5LIFE and 1.5TECH scenarios, which foresees net-zero greenhouse gas emissions by 2050. Whereas 1.5LIFE assumes changing business and

4 Stiftung Offshore (2017), IEA (2019)

5 ASSET (2018). In 2018, the global weighted average capacity factor for offshore wind amounted to 43%, i.e. nearly 3,800 full-load hours (IRENA 2019).

6 IRENA (2019)

7 IEA (2019), IRENA (2019)



consumption patterns towards a more circular economy, 1.5TECH features a stronger role for biomass and carbon capture and storage. The total power generation capacity in the two 1.5 scenarios ranges from around 2,300 GW to 2,800 GW in 2050, with the share of renewables in gross electricity generation reaching more than 80% and – within renewables – wind representing the dominating renewable energy technology (>50%).⁸

Offshore wind reaches an installed capacity of 396 GW by 2050 in the 1.5LIFE scenario and of 451 GW in the 1.5TECH scenario (see Figure 2), up from around 20 GW installed in the EU today.⁹

Deploying 450 GW of offshore wind in all over Europe would require a considerable increase in the annual installation rate, starting from around 3 GW today to some 7 GW by the second half of the 2020s and to over 20 GW per year by the mid 2030s.¹⁰

Additional demand of up to 500 GW may be created by dedicating offshore farms to electrolysis for renewable hydrogen production.

Electrolysers for hydrogen production are economically most efficient when operated on a continuous basis. Efficient green hydrogen production thus requires a renewable energy source that can deliver many full-load hours, a requirement that is well suited to offshore wind.¹¹ As a result, offshore wind deployment goes hand in hand with greater hydrogen production in many scenarios. For example, the “optimized gas scenario”, commissioned by the “Gas for Climate” group, projects total installed offshore wind capacity of 1010 GW in order to achieve

net-zero EU emissions in 2050. Half of this capacity is dedicated to green hydrogen production.¹² When producing green hydrogen, offshore wind will compete with exceptionally inexpensive solar PV and onshore wind at very good sites around the globe. However, given the high transport costs associated with long-distance hydrogen shipping – whether as liquid hydrogen, ammonia, or in liquid organic hydrogen carriers – offshore wind located in Europe might have a competitive advantage.¹³

8 EC (2018b)

9 IEA (2019)

10 Wind Europe (2019)

11 Agora Verkehrswende, Agora Energiewende and Frontier Economics (2018)

12 Navigant (2019). According to the authors, the “optimized gas scenario” resembles the 1.5TECH scenario. Electrolysis can be implemented onshore or offshore (Tractebel 2019). The former requires a grid connection to an offshore wind park, the latter involves hydrogen transport from the offshore farm to the mainland, which could be realized through pipelines or specialized vessels (Navigant 2019, E-Bridge 2018, IEA 2019).

13 Agora Energiewende (2019), Agora Verkehrswende, Agora Energiewende and Frontier Economics (2018)

2

Scenarios projecting near climate neutrality by 2050 assume an installed capacity of 50 to 70 GW of offshore wind in Germany, generating some 200 to 280 TWh of electricity per year.

In recent years, a total of 8 GW of offshore wind capacity has been installed in the German section of the North Sea (Figure 3). For 2050, climate target scenarios with a reduction in greenhouse gases of 95% relative to 1990 show installed offshore wind capacity ranging between 50 and 70 GW. To reach such capacities by 2050, a gross capacity of about 1 to 2 GW of offshore wind would need to be installed per year.

Whether onshore or offshore, wind power plays a decisive role in the deep decarbonization scenarios that have been developed for Germany, as the generation profile of wind is especially well suited to cover

demand from heating during the winter season. Depending on a variety of assumptions, including future hydrogen requirements and fuel imports, total electricity generation from wind energy in 2050 is projected to range between 470 and 750 TWh per year (Figure 4). Of this amount, 220 to 520 TWh could potentially be generated by onshore wind, and 180 to 280 TWh by offshore wind.¹⁴ These ranges show that within certain bounds, onshore wind can act as a substitute for offshore wind, despite widely divergent transmission grid requirements. The expansion of

14 Acatech et al. (2017), Agora Energiewende (2020), BDI (2018), BMU (2015), MWV (2018)

Installed offshore wind capacity for Germany's 95 % climate target scenarios in GW

Figure 3

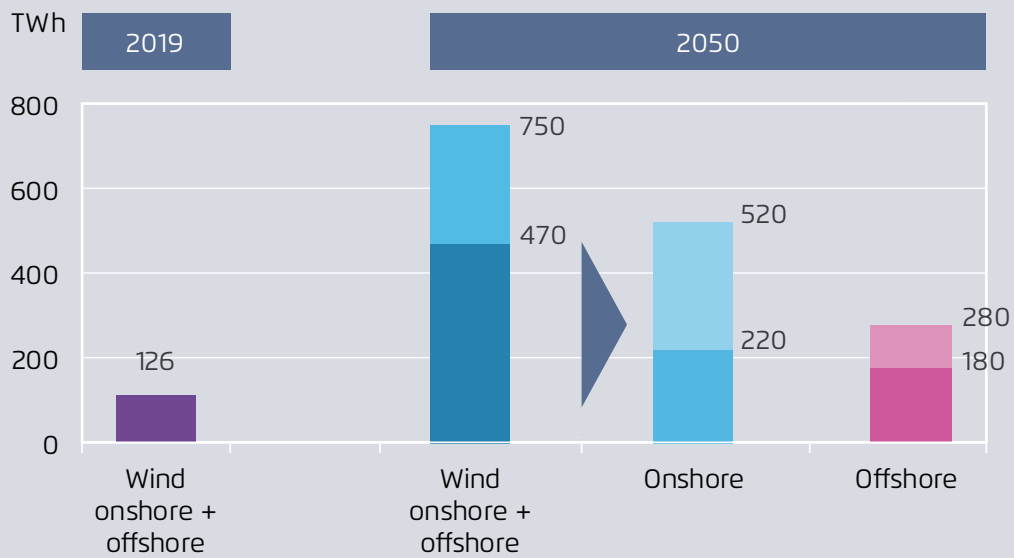


Note: Acatech models a greenhouse gas emission reduction of 90% relative to 1990 by 2050. This diagram does not include installed capacities for 2050 of around 30 GW as shown in Dena (2018), because those scenarios include an unusually high volume of imported renewable hydrogen and e-fuels.

Acatech et al. (2017), Agora Energiewende (2020), BDI (2018), BMU (2015), MWV (2018), Stiftung Offshore (2017)

Ranges of necessary wind power generation by 2050 in 95% decarbonization scenarios for Germany in TWh

Figure 4



Note: Figures are rounded; Acatech et al. models a 90% GHG emission reduction by 2050

Acatech et al. (2017), Agora Energiewende (2020), BDI (2018), BMU (2015), MWV (2018)

offshore wind will primarily take place in northern Germany, thus augmenting the need for grid connections to the south. Onshore wind, on the other hand, can be spread out more evenly across Germany. Due to its very different seasonal profile, solar PV can only partially act as a substitute for wind energy.

Given the 8 GW of installed capacity today and current plans for 20 GW by 2030, the pace of spatial planning for offshore wind deployment needs to pick up significantly.

From 2008 to 2019, Germany installed offshore wind capacity at an average rate of 0.7 GW per year (Table 1).

Offshore wind growth in Germany: Past expansion and future requirements in GW

Table 1

| Scenario range 2050 | Installed capacity in GW | | | | Capacity addition in GW per year | | |
|---------------------|--------------------------|------|------|------|----------------------------------|-------------|-------------|
| | 2008 | 2019 | 2030 | 2050 | 2008 – 2019 | 2019 – 2030 | 2030 – 2050 |
| Lower end | 0 | 8 | 20 | 45 | 0.7 | 1.1 | 1.3 |
| Upper end | | | | 70 | | | 2.5 |

Agora Energiewende (2020), Bundesregierung (2019), BMU (2015), MWV (2018)

Reaching the new target of 20 GW by 2030¹⁵ implies an increase of this installation rate to around 1.1 GW per year. After 2030, annual deployment would only need to be slightly higher (1.3 GW/a) to reach 45 GW, the lower end of the scenario range for wind capacity in 2050. By contrast, achieving the higher end of 70 GW would involve more than a doubling of annual deployment to 2.5 GW per year from 2030 to 2050.

The slowing of onshore wind development could further enhance the importance of offshore wind in achieving net zero.

For years, a generally accepted assumption in discussions about the German energy transition has been that reserving 2 % of national territory for onshore wind turbines is a realistic benchmark.¹⁶ However, this basic assumption is now being challenged by policy-makers in Germany who demand general minimum distances between wind turbines and inhabited areas. Troublingly, increasing the general minimum distance to 1000 m would reduce the areas suitable for onshore wind development by 20 to 50 per cent.¹⁷ Conversely, reducing minimum distances to 600 m would allow onshore wind energy to play a much larger role in the German energy transition.¹⁸

In addition to land availability issues, onshore wind expansion is being impaired by a lack of evidence-based standards and procedures in the area of nature conservation.¹⁹ As a consequence, the first

nine months of 2019 saw the lowest onshore wind installation rate in Germany of the last 20 years.²⁰ With onshore wind expansion in Germany currently falling short of long-term climate targets, some policy-makers have argued that expanded deployment of offshore wind could act as a substitute for onshore wind, and that the current “expansion corridor” should be adjusted correspondingly.²¹ While both turbine types have similar generation profiles²², there remains a major difference: Onshore wind turbines can be erected in close proximity to demand centres all over Germany, whereas offshore wind energy needs to be transported over considerable distances, thus necessitating an offshore grid connection and sufficient onshore transmission capacity.²³

15 As announced by the German Federal Government in its Climate Action Programme 2030 (Bundesregierung 2019). In addition, the heads of governments in northern German states have recently demanded the construction of 30 GW of offshore turbines by 2035 (Niedersächsische Staatskanzlei 2019).

16 BWE (2012)

17 UBA (2019)

18 IASS (2019)

19 BDEW et al. 2019; BMWI 2019

20 Fachagentur Wind (2019)

21 Stratmann (2019)

22 See page 9 for details on differences between onshore and offshore wind.

23 The IEA (2019) underlines that “additional investment in onshore transmission is key to making the most of offshore wind”.

3

Offshore wind power needs sufficient space, as the full load operating time may otherwise shrink from currently around 4,000 hours per year to between 3,000 and 3,300 hours.

Energy scenarios for the EU assume future generation of 4,000 to 5,000 full-load hours at very good offshore wind sites.²⁴ The analysis presented in this publication, however, describes considerable reductions in full load hours for the German section of the North Sea. This finding is derived from using two methods that differ substantially in complexity, with one ("KEBA") being simple and fast, and the other ("WRF") being highly detailed and requiring a computer cluster to perform the simulations.²⁵ Nevertheless, both methods show a remarkable level of agree-

ment in the overall magnitude of yield reductions. Figure 5 illustrates how the full-load hours achievable by offshore wind farms decrease as the area covered by the turbines expands, ranging from a comparatively small to a large reduction.

If Germany were to install 28 GW of wind turbines in an area of around 2,800 km² in the German Bight only, the yield would fall to around 3,400 full-load hours, corresponding to nearly 100 TWh of electricity.²⁶ Installing 72 GW of turbines in an area of about 7,200 km² exclusively in the German Bight would further reduce full-load hours to about 3,000 hours

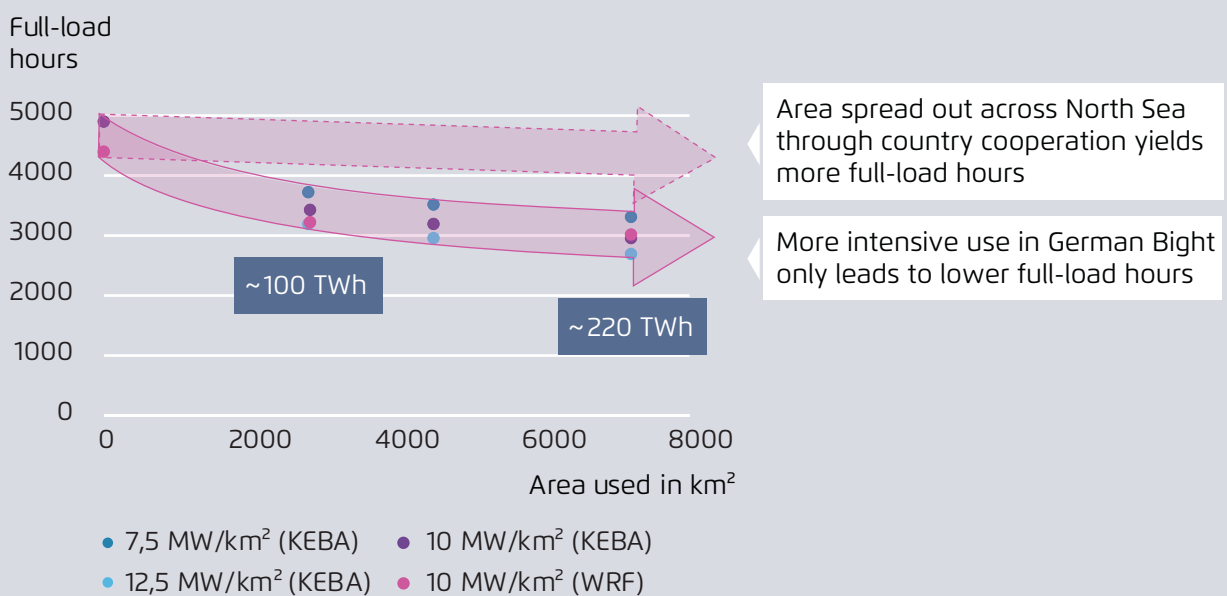
24 See figure 1.

25 KEBA: Kinetic Energy Budget of the Atmosphere. WRF: Weather Research and Forecast model. For details, see part II of this publication.

26 The 2,800 km² refer to the near-shore coastal areas defined as O-NEP zones 1 to 3 (BSH 2019b).

Full-load hours achievable depending on area for offshore wind deployment in the North Sea (and expected yield in TWh)

Figure 5



Authors' figure, based on DTU and MPI-BGC (2020)

per year, yielding approximately 220 TWh of electricity. As an alternative, the wind farms could be spread out over a larger area on the basis of cooperation with other countries. This would considerably augment the number of achievable full-load hours, according to our estimations.

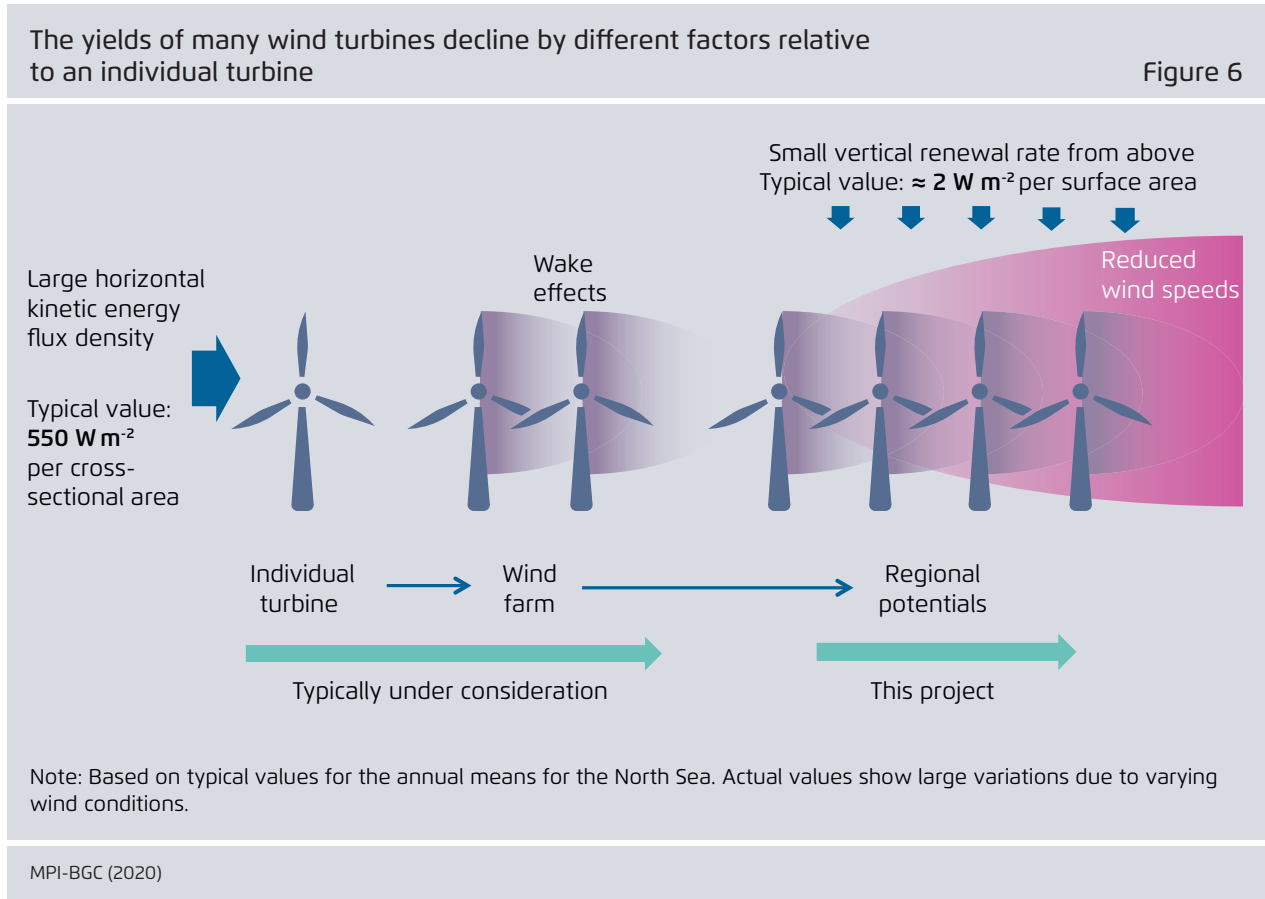
The more turbines are installed in a region, the less efficient offshore wind production becomes due to a lack of wind recovery.

Wind turbines convert kinetic energy from the atmosphere into electricity, thereby reducing wind speeds.²⁷ Mean wind speed reductions behind the turbine, together with increased turbulence levels, are

27 In addition, they also lead to dissipation of kinetic energy through friction.

called “wakes”.²⁸ By mixing with the surrounding air flow, depleted winds are replenished. In this way, wind farm planners and investors must necessarily consider wake effects between individual turbines and entire wind farms (see Figure 6). As the size of the region under consideration increases, it is also important to take the overall reduction of kinetic energy of the regional air flow into account: The more

28 Wakes recover mainly through atmospheric turbulence. Over land, the heating of the earth’s surface by sunlight as well as natural and man-made surface roughness generate turbulence, leading to shorter wakes of a few kilometres in length at most. Over sea, heating by solar radiation takes place below the surface, causing less heating at the surface. Additionally, water surfaces are less contoured, meaning less turbulence but considerably longer wakes. Simulations predict wakes of up to 100 km, and empirical measurements have shown wakes to reach at least 45 km in length (Platis et al. 2018).



the surrounding horizontal air flow is affected, the greater the reduction in downstream wind speeds, because additional kinetic energy can effectively only come from higher atmospheric layers, and the vertical renewal rate from above is limited.²⁹ Accordingly, the analysis presented in this publication considers wake effects, including large-scale wind flow impacts.

The impact of the kinetic energy removal increases in line with the size of the wind farm and spatial density of the turbines. This general phenomenon is more relevant in the offshore setting than for onshore wind due to divergence in surface roughness, surface heating and the density of turbine capacity.

Over land, the natural and man-made surface roughness caused by vegetation, mountains and buildings leads to lower wind speeds than over the sea.³⁰ At the same time, surface obstacles produce stronger turbulence and the mixing of air flows, which is further enhanced by solar heating during the day, implying shorter wake effects onshore than offshore.

Wind turbine capacity densities in Germany differ considerably between onshore and offshore wind power. While planned offshore densities are on the order of 10 MW/km²,³¹ actual onshore densities in 2018 averaged below 0.5 MW/km² when looking at individual German states.³² Given this large differ-

ence and the divergence in air flow stability described above, onshore wind turbines in Germany are less likely to experience relevant reductions in achievable full-load hours anytime soon.³³ However, given the long-run target of generating 220 to 520 TWh electricity from onshore wind in Germany³⁴, further research on this question is warranted. Similarly, work should be conducted to understand the potential effects of offshore wind farms on their downstream onshore counterparts.

29 The typical values shown in Figure 6 are based on typical annual means for the North Sea, but the actual values show large variation due to varying wind conditions. Note that the magnitude of the vertical renewal rate is limited by the comparatively low generation rate of kinetic energy generation rate of the atmosphere, which is governed by the dynamics and thermodynamics of the atmosphere.

30 Quaschnig (2005)

31 BSH (2019b)

32 Schleswig-Holstein had 0.4 MW/km²; other northern states around 0.3 MW/km²; southern states below 0.05 MW/km². Yet when looking at individual postal code areas, some capacity densities reach up to the 5 MW/km² scale (Fh-IEE 2019).

33 In fact, such reductions could not be detected in an analysis covering 2000–2014 (Germer und Kleidon 2019). In addition, a countervailing effect may be the observed reversal of global terrestrial stilling (Zeng et al. 2019).

34 See Figure 4 above.

If Germany were to install 50 to 70 GW solely in the German Bight, the number of full-load hours achieved by offshore wind farms would decrease considerably.

Today, state planning for future offshore wind deployment in the German Bight is based on national maritime spatial planning and site development plans, implemented by the Federal Maritime and Hydrographic Agency (BSH). Its mandate ends at the borders of the German Exclusive Economic Zone. However, installing 50 to 70 GW solely in the German section of the North Sea would reduce full-load hours considerably and make offshore wind generation markedly more expensive than originally assumed.

4

Countries on the North and Baltic Seas should cooperate with a view to maximizing the wind yield and full-load hours of their offshore wind farms.

To date, spatial planning for offshore wind development has generally had a national focus.³⁵ The analysis presented in this publication, however, underscores the need for more coordination to efficiently exploit offshore wind resources in Europe as a whole. A key aspect of this analysis is its extended notion of wakes to explicitly include the removal of kinetic energy from regional air flow. The findings indicate that offshore wind farm development must consider regional wind dynamics. Specifically, due attention must be given to the reductions in wind speeds and yields that occur when wind farms are constructed in close proximity to one another. By extension, sufficiently large spaces between wind farms should be preserved in order to ensure replenishment of wind speeds. These replenishment areas could potentially be reserved for other purposes, such as shipping corridors or nature conservation. The understanding of regional wind impacts presented in this publication is particularly relevant with a view to the cross-border effects of kinetic energy removal, given the potential for wind depletion beyond national boundaries.

In order to maximize the efficiency and potential of offshore wind, the planning and development of wind farms – as well as broader maritime spatial planning – should be intelligently coordinated across national borders.

In light of the foregoing discussion, broader maritime spatial planning is an important part of large-scale least-cost offshore wind development. Aside from the kinetic energy removal effect, key cost factors include the water depth and distance to shore. The EU Directive on Maritime Spatial Planning obliges coastal Member States to develop national maritime

spatial plans by 2021, to coordinate those plans with each other, and to take other transnational issues into account.³⁶ Despite this requirement for cooperation, the cross-border removal of kinetic energy has yet to be systematically addressed. Such issues should be incorporated into the envisaged offshore wind strategy and regional cooperation as part of the European Green Deal.³⁷

Projects that are connected to more than one country via an offshore electricity interconnector could represent a compelling opportunity within the scope of offshore wind planning and development. Such interconnections could serve as the springboard for the development of an offshore meshed grid, and could take different forms, including combined grid solutions or offshore hubs.³⁸ The “hub-and-spoke” model that has been proposed for North Sea Wind Power Hub is one prominent example of a solution in this area. This consortium has examined four locations,³⁹ as shown in Figure 7: (1) the Dutch Exclusive Economic Zone (EEZ) on the Dogger Bank; (2) the Dutch EEZ south of Dogger Bank; (3) the Danish EEZ

35 NSWPH (2019a)

36 Directive 2014/89/EU. The European Union itself has no general competence assigned within the field of spatial planning. However, it provides support, e.g. through the European Maritime Spatial Planning Platform <https://www.msp-platform.eu> (BSH 2019a).

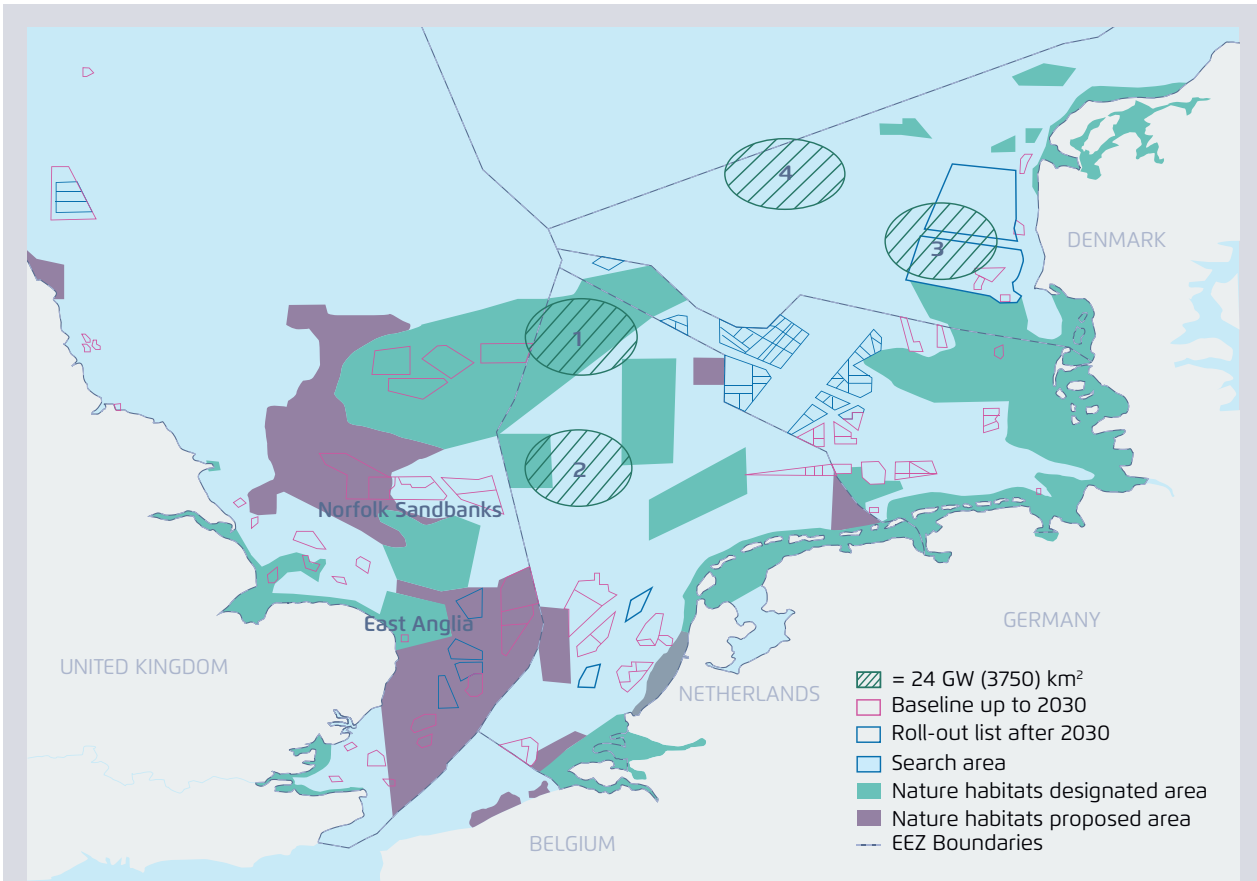
37 EC (2019a, b)

38 Referred to as “hybrid projects” by Wind Europe (2019: 44). Hybrid offshore wind farms do not exist so far, except for the Kriegers Flak project, which has been in the making for 10 years (Wind Europe 2019).

39 Those locations do not represent preferences for the location of an initial project. Rather, they have been used to test location-specific impacts on hub-and-spoke design (NSWPH 2019b).

Four illustrative areas for the development of offshore wind hubs in the North Sea

Figure 7



Note: Those locations do not represent preferences for the location of an initial project. Rather, they have been used to test location-specific impacts on hub-and-spoke design.

NSWPH (2019b)

west of Jutland; and (4) a location in the deeper part of the Danish EEZ and part of the Norwegian EEZ.⁴⁰

Our findings are relevant to both the North and Baltic Seas.

While the analysis presented in this publication is only concerned with the German section of the North Sea, it clearly has relevance for other waters as well, including the Baltic Sea. With an estimated potential of more than 200 GW, the North Sea is the body of water with the largest offshore potential for Europe. Nevertheless, the Baltic Sea’s potential is estimated at more than 80 GW.⁴¹

40 The analysis includes the option of power-to-hydrogen conversion. It also finds significant increases in losses due to wake and blockage effects (NSWPH 2019b). Another example is Oersted’s recently unveiled plan for a 5 GW offshore wind hub connecting several countries in the Baltic Sea and including the option of hydrogen production (Recharge 2019).

41 Wind Europe (2019)

Floating offshore wind farms could enable the creative integration of deep waters into wind farm planning.

Traditional fixed-bottom offshore wind installations are typically installed in water depths of less than 50 to 60 meters due to the high costs associated with increasing water depth, which can quickly make the plants uneconomical.⁴² The relatively new technology of floating offshore foundations promises to overcome this limitation and open up new areas to offshore wind development that would otherwise be practically inaccessible.⁴³ Indeed, the European deployment scenario, which projects 450 GW of installed offshore wind capacity by 2050, already assumes 100 to 150 GW of floating offshore wind capacity.⁴⁴ Yet continued deployment at scale is required to achieve further cost reductions and enable floating foundations to play a meaningful role in the future.⁴⁵

42 IEA (2019)

43 It also holds the promise of greater ease of turbine set-up, potentially lower future costs, and greater environmental benefits due to less invasive activity on the seabed during installation (IRENA 2019). Still, floating offshore wind will also need to consider the impact of large scale wake effects, including the overall reduction of kinetic energy on the regional air flow, as described in this publication.

44 Wind Europe (2019)

45 Currently, the only successful operational large-scale floating wind farm is the 30 MW Hywind project in Scotland. A much larger project recently received approval for installing 200 MW of floating turbines off the coast of the Canary Islands. This would be the world's largest when starting operation in the mid-2020s (IRENA 2019, IEA (2019)).

References

- Acatech et al. (2017):** Acatech, Leopoldina, Akademiunion. "Sektorkopplung" – Untersuchungen und Überlegungen zur Entwicklung eines integrierten Energiesystems, Analyse, November 2017 (Schriftenreihe Energiesysteme der Zukunft)
https://energiesysteme-zukunft.de/fileadmin/user_upload/Publikationen/PDFs/ESYS_Analyse_Sektorkopplung.pdf
- Agora Energiewende (2017):** Wärmewende 2030. Schlüsseltechnologien zur Erreichung der mittel- und langfristigen Klimaschutzziele im Gebäudesektor. Fh-IWES/IBP.
https://www.agora-energiewende.de/fileadmin2/Projekte/2016/Sektoruebergreifende_EW/Waermewende-2030_WEB.pdf
- Agora Energiewende (2019):** EU-wide innovation support is key to the success of electrolysis manufacturing in Europe. Background.
https://www.agora-energiewende.de/fileadmin2/Blog/2019/Electrolysis_manufacturing_Europe/2019-11-08_Background_paper_Hydrogen_cost.pdf
- Agora Energiewende (2020):** Die Energiewende im Stromsektor: Stand der Dinge 2019. Rückblick auf die wesentlichen Entwicklungen sowie Ausblick auf 2020.
https://www.agora-energiewende.de/fileadmin2/Projekte/2019/Jahresauswertung_2019/171_A-EW_Jahresauswertung_2019_WEB.pdf
- Agora Verkehrswende, Agora Energiewende and Frontier Economics (2018):** The Future Cost of Electricity-Based Synthetic Fuels,
https://www.agora-energiewende.de/fileadmin2/Projekte/2017/SynKost_2050/Agora_SynKost_Study_EN_WEB.pdf
- ASSET (2019):** Technology pathways in decarbonisation scenarios, Advanced System Studies for Energy Transition, July 2018,
https://ec.europa.eu/energy/sites/ener/files/documents/2018_06_27_technology_pathways_-_finalreportmain2.pdf
- BDEW et al. (2019):** 10 Punkte für den Ausbau der Windenergie. Vorschläge zur Gewährleistung von Flächenverfügbarkeit, Handhabbarkeit naturschutzrechtlicher Vorgaben und Stärkung vor Ort. Berlin, 3. September 2019.
https://www.bdew.de/media/documents/Stn_20190903_10-Punktefuer-Ausbau-Windenergie-Verbaende.pdf
- BDI (2018):** Klimapfade für Deutschland. BCG, Prognos, commissioned by Bundesverband der Deutschen Industrie (BDI),
<https://bdi.eu/themenfelder/energie-und-klima/klima2050/>
- BMU (2015):** Klimaschutzszenario 2050. 2. Endbericht, Öko-Institut, Fh-ISI, commissioned by Bundesministerium für Umwelt (BMU).
www.oeko.de/oekodoc/2451/2015-608-de.pdf
- BMWi (2019):** Windenergie an Land. Aufgabenliste zur Schaffung von Akzeptanz und Rechtssicherheit für die Windenergie an Land, Berlin, den 7. Oktober 2019,
https://www.bmwi.de/Redaktion/DE/Downloads/S-T/staerkung-des-ausbaus-der-windenergie-an-land.pdf?__blob=publicationFile&v=12
- BSH (2019a):** International spatial planning. The importance of European cooperation in maritime spatial planning, Bundesamt für Seeschifffahrt und Hydrographie,
https://www.bsh.de/EN/TOPICS/Offshore/Maritime_spatial_planning/International_spatial_planning/international_spatial_planning_node.html
-

BSH (2019b): *Flächenentwicklungsplan 2019 für die deutsche Nord- und Ostsee*. 28.06.2019, Bundesamt für Seeschifffahrt und Hydrographie, https://www.bsh.de/DE/PUBLIKATIONEN/_Anlagen/Downloads/Offshore/FEP/Flaechenentwicklungsplan_2019.pdf?__blob=publicationFile&v=8

Bundesregierung (2019): *Climate Action Programme 2030. An overview*. <https://www.bundesregierung.de/breg-en/issues/climate-action/klimaschutzprogramm-2030-1674080>

BWE (2012): *Potenzial der Windenergienutzung an Land*, Kurzfassung, Bundesverband Windenergie, https://www.wind-energie.de/fileadmin/redaktion/dokumente/publikationen-oeffentlich/themen/01-mensch-und-umwelt/03-naturschutz/bwe_potenzialstudie_kurzfassung_2012-03.pdf

Dena (2018): *Dena-Leitstudie Integrierte Energiewende. Impulse für die Gestaltung des Energiesystems bis 2050*, ewi Energy Research & Scenarios, commissioned by Deutsche Energie-Agentur (dena), https://www.dena.de/fileadmin/dena/Dokumente/Pdf/9261_dena-Leitstudie_Integrierte_Energiewende_lang.pdf

E-Bridge (2018): *Wasserstoffherzeugung in Kombination mit Offshore-Windausbau*. https://www.e-bridge.de/wp-content/uploads/2018/12/20181204_E-Bridge_H2_OffshoreWind_final_Studie_gesamt-1.pdf

EC (2018a): Communication from the Commission to the European Parliament, the European Council, the Council, the European Economic and Social Committee, the Committee of the Regions and the European Investment Bank. *A Clean Planet for all. A European strategic long-term vision for a prosperous, modern, competitive and climate neutral economy*. European Commission, COM(2018) 773 final, <https://eur-lex.europa.eu/legal-content/EN/TXT/?uri=CELEX:52018DC0773>

EC (2018b): In-Depth Analysis in Support of the Commission Communication COM(2018) 773. *A Clean Planet for all. A European strategic long-term vision for a prosperous, modern, competitive and climate neutral economy*. European Commission, https://ec.europa.eu/clima/sites/clima/files/docs/pages/com_2018_733_analysis_in_support_en_0.pdf

EC (2018c): Supplementary information. In-Depth Analysis in Support of the Commission Communication COM(2018) 773. *A Clean Planet for all. A European strategic long-term vision for a prosperous, modern, competitive and climate neutral economy*. European Commission

EC (2019a): Communication from the Commission to the European Parliament, the European Council, the Council, the European Economic and Social Committee and the Committee of the Regions. *The European Green Deal*. European Commission. COM (2019) 640 final.

EC (2019b): Annex to the Communication from the Commission to the European Parliament, the European Council, the Council, the European Economic and Social Committee and the Committee of the Regions. *The European Green Deal*. European Commission. COM (2019) 640 final.

FA Wind (2019): *Ausbausituation der Windenergie an Land im Herbst 2019. Auswertung windenergiespezifischer Daten im Marktstammdatenregister für den Zeitraum Januar bis September 2019*. Fachagentur Wind (2019).

https://www.fachagentur-windenergie.de/fileadmin/files/Veroeffentlichungen/Analysen/FA_Wind_Zubauanalyse_Wind-an-Land_Herbst_2019.pdf

Fh-IEE (2019): *Windenergie Report Deutschland 2018*, Fraunhofer-Institut für Energiewirtschaft und Energiesystemtechnik (IEE), http://windmonitor.iee.fraunhofer.de/opencms/export/sites/windmonitor/img/Windmonitor-2018/WERD_2018_barrierefrei.pdf

Germer, Sonja, und Axel Kleidon (2019): *Have Wind Turbines in Germany Generated Electricity as Would Be Expected from the Prevailing Wind Conditions in 2000-2014?* PLOS ONE 14 (2): e0211028.
<https://doi.org/10.1371/journal.pone.0211028>

IASS (2019): *Ohne Windenergie keine Energiewende. Die 1000 Meter-Abstandsregelung macht Windenergieausbau unmöglich und stellt damit den Kohleausstieg in Deutschland in Frage. Analyse und Einschätzung der Konsequenzen für die Ausbauziele der Bundesregierung*, Institute for Advanced Sustainability Studies,
https://www.iass-potsdam.de/sites/default/files/2019-11/Discussion%20Paper_MindestabstandWindkraftanlagen_published_22112019.pdf

IEA (2019): *Offshore Wind Outlook 2019*. World Energy Outlook Special Report, International Energy Agency,
<https://www.iea.org/reports/offshore-wind-outlook-2019>

IRENA (2019): *Future of wind. Deployment, investment, technology, grid integration and socio-economic aspects. A Global Energy Transformation paper*.
https://www.irena.org/-/media/Files/IRENA/Agency/Publication/2019/Oct/IRENA_Future_of_wind_2019.pdf

MWV (2018): *Status und Perspektiven flüssiger Energieträger in der Energiewende*. Prognos AG, Fh-UMSICHT, DBFZ, commissioned by Mineralölwirtschaftsverband e.V. (MWV), IWO, MEW, UNITI,
https://www.mwv.de/wp-content/uploads/2018/06/Prognos-Endbericht_Fluessige_Energietraeger_Web-final.pdf

Navigant (2019): *Gas for Climate. The optimal role for gas in a net-zero emissions energy system*. Prepared for Gas for Climate.

https://www.gasforclimate2050.eu/files/files/Navigant_Gas_for_Climate_The_optimal_role_for_gas_in_a_net_zero_emissions_energy_system_March_2019.pdf

Niedersächsische Staatskanzlei (2019): *Wirklicher Klimaschutz nur mit Windenergie aus dem Norden*, 29 November 2019,

<https://www.stk.niedersachsen.de/startseite/presseinformationen/wirklicher-klimaschutz-nur-mit-windenergie-aus-dem-norden-183105.html>

NSWPH (2019a): *Requirements to build. Post-2030 planning is needed now*, North Sea Wind Power Hub,
https://northseawindpowerhub.eu/wp-content/uploads/2019/07/NSWPH-1903-Concept_Paper_6-Build-v04.pdf

NSWPH (2019b): *Modular hub-and-spoke: Specific solution options*. North Sea Wind Power Hub. June 2019.

https://northseawindpowerhub.eu/wp-content/uploads/2019/07/Concept_Paper_3-Specific-solution-options.pdf

Quaschnig (2005): *Understanding Renewable Energy Systems*, Earthscan

Recharge (2019): *Orsted plans 'world first' 5GW offshore wind energy island*. 25 November 2019.
<https://www.rechargenews.com/wind/orsted-plans-world-first-5gw-offshore-wind-energy-island/2-1-712332>

Stiftung Offshore (2017): *Energiewirtschaftliche Bedeutung der Offshore-Windenergie für die Energiewende*. Update 2017, Fh-IWES, commissioned by Stiftung Offshore Windenergie
https://www.offshore-stiftung.de/sites/offshorelink.de/files/documents/Studie_Energiewirtschaftliche%20Bedeutung%20Offshore%20Wind.pdf

Stratmann (2019): *Offshore-Windbranche will schneller wachsen.* In: Handelsblatt Online, 09.08.2019, <https://www.handelsblatt.com/politik/deutschland/energiewende-offshore-windbranche-will-schneller-wachsen/24885448.html>

Tractebel (2019): *Offshore-Wasserstoff-Produktion mit 400 MW in neuer Dimension.* 1 October 2019. <https://tractebel-engie.de/de/nachrichten/2019/offshore-wasserstoff-produktion-mit-400-mw-in-neuer-dimension>

UBA (2019): *Auswirkungen von Mindestabständen zwischen Windenergieanlagen und Siedlungen. Auswertung im Rahmen der UBA-Studie „Flächenanalyse Windenergie an Land“.* Umweltbundesamt. Position. März 2019, https://www.umweltbundesamt.de/sites/default/files/medien/1410/publikationen/2019-03-20_pp_mindestabstaende-windenergieanlagen.pdf

Wind Europe (2019): *Our energy, our future. How offshore wind will help Europe go carbon-neutral,* <https://windeurope.org/wp-content/uploads/files/about-wind/reports/WindEurope-Our-Energy-Our-Future.pdf>

Zeng, Zhenzhong et al. (2019): *A Reversal in Global Terrestrial Stilling and Its Implications for Wind Energy Production.* Nature Climate Change 9 (12): 979–85. <https://doi.org/10.1038/s41558-019-0622-6>

Making the Most of Offshore Wind: Re-Evaluating the Potential of Offshore Wind in the German North Sea

Please cite as:

Technical University of Denmark and Max-Planck-Institute (2020): Making the Most of Offshore Wind: Re-Evaluating the Potential of Offshore Wind in the German North Sea. Study commissioned by Agora Energiewende and Agora Verkehrswende.

In: Agora Energiewende, Agora Verkehrswende, Technical University of Denmark and Max-Planck-Institute for Biogeochemistry (2020): Making the Most of Offshore Wind: Re-Evaluating the Potential of Offshore Wind in the German North Sea.

1 Summary

Introduction and background

Existing climate **target scenarios for Germany** to reduce GHG emissions by 95% by 2050 relative to 1990 include installed offshore wind capacities in the range of 30 to 70 GW. Yet, the size of offshore regions that Germany administers is relatively small. They are located primarily in the North Sea, and in border regions administered by neighbouring countries that also intend to develop offshore wind energy.

Prior research suggests that when wind energy is used at larger scales, the efficiency of wind turbines is reduced due to atmospheric effects, resulting in lower capacity factors and fewer full-load hours. Current energy scenarios, however, typically assume an increase in turbine efficiencies, as expressed by capacity factor or full-load hours, due to technological developments. Typically, modellers assume around 4,000 to 5,000 full-load hours for the future.

The goal here is to **evaluate the relevance of atmospheric effects** in reducing yields in realistic scenarios of offshore wind energy development in the North Sea, using two methods that differ in their complexity. The focus is to evaluate yields that go beyond the typical wake effects that are observed and considered in wind farms.

Wake effects are found behind the wind turbine rotors and the depleted winds are replenished by the surrounding flow. An incomplete replenishment results in a reduced yield of downwind turbines. This effect is well studied and understood and regularly included in yield estimates for wind farms. Yet, it is assumed that the surrounding flow is not affected. Our focus here is to include this effect on the surrounding flow, by evaluating the overall **reduction of kinetic energy of the regional air flow** in regional scenarios of offshore wind energy use.

Goals and scenarios

This project evaluates a set of offshore scenarios with total installed capacities of offshore wind power ranging from 14 to 145 GW. We have focused these scenarios on the German section of the Exclusive Economic Zone (EEZ) of the North Sea, as it contains the majority of regions suitable for offshore wind energy in Germany. We use the characteristics of a hypothetical 12 MW turbine ("BSH-200-P12"), different densities of installed capacity, ranging from 5 MW/km² to 20 MW/km², and different areas. This yields a range of total installed **capacities from 14 GW to 145 GW**, corresponding to a total of about 1,200 to 12,000 turbines with 12 MW each.

Methods

We use two methods to estimate wind speed reductions using descriptions of the atmospheric flow surrounding the wind farm regions:

KEBA: Kinetic Energy Budget of the Atmosphere. This method uses the kinetic energy budget of the atmosphere surrounding the wind farms to diagnose wind speed reductions due to the removal by wind turbines and simultaneously estimates energy yields.

WRF: Weather Research and Forecast model. The WRF model is a numerical weather prediction model of the kind that is used by weather forecasting centres and researcher all over the world. In this model, the influence of wind turbines is represented through Explicit Wake Parameterization.

The two methods differ substantially in complexity, with KEBA being simple and fast, and WRF being highly detailed and requiring a computer cluster to perform the simulations.

Results

Both methods show an increasing yield reduction effect with larger installed capacities, ranging from a comparatively small reduction to a large reduction by

more than 50% (see Table 1 below). For example, in the case of 72 GW installed with a density of 10 MW/km², the simulations yield around **3,000 full-load hours**.

Summary of results from the KEBA and WRF simulations

Table 1

| Formulation of scenarios | | | | Results | | | | | |
|---|--------------------------|--------------------------|-------------------------------|--|------|------------------------|-------|-------------------------|------|
| Density (W/m ² or MW/km ²) | Included areas | | Installed capacity (GW) | With wakes caused by kinetic energy removal | | | | | |
| | Area 1 | Area 2 | | Yield (GW) | | Full-load hours [h] | | Capacity factor* [%] | |
| | 2,767 km ² | 4,473 km ² | | WRF | KEBA | WRF | KEBA | WRF | KEBA |
| | | | | | | | | | |
| 5 | x | | 13.8 | 6.0 | 6.4 | 3,770 | 4,065 | 43 % | 46 % |
| 5 | | x | 22.4 | | 10.0 | | 3,913 | | 45 % |
| 5 | x | x | 36.2 | 15.3 | 15.4 | 3,693 | 3,729 | 42 % | 43 % |
| 7.5 | x | | 20.8 | | 8.8 | | 3,713 | | 42 % |
| 7.5 | | x | 33.5 | | 13.5 | | 3,530 | | 40 % |
| 7.5 | x | x | 54.3 | 20.8 | 20.5 | 3,348 | 3,309 | 38 % | 38 % |
| 10 | x | | 27.7 | 10.3 | 10.9 | 3,255 | 3,449 | 37 % | 39 % |
| 10 | | x | 44.7 | | 16.4 | | 3,216 | | 37 % |
| 10 | x | x | 72.4 | 25.1 | 24.5 | 3,040 | 2,966 | 35 % | 34 % |
| 12.5 | x | | 34.6 | | 12.6 | | 3,190 | | 36 % |
| 12.5 | | x | 55.9 | | 18.8 | | 2,949 | | 34 % |
| 12.5 | x | x | 90.5 | 28.7 | 27.7 | 2,776 | 2,683 | 32 % | 31 % |
| 20 | x | | 55.3 | | 16.4 | | 2,600 | | 30 % |
| 20 | | x | 89.5 | | 23.8 | | 2,331 | | 27 % |
| 20 | x | x | 144.8 | 36.0 | 34.2 | 2,179 | 2,070 | 25 % | 24 % |

* Other losses not included.

DTU and MPI-BGC (2020)

Interpretation

Both methods show a **remarkable level of agreement** regarding the overall magnitude of yield reductions caused by the wind turbines. As both models capture reduction effects on wind speeds that are caused by

the removal of kinetic energy through wind-turbine operation, these estimates show that a very large-scale and dense deployment of wind turbines in the North Sea region is likely to cause significant effects on the wind field within the region, resulting in lower yields.

The reason for the yield reductions can be understood by the atmospheric flows of kinetic energy. The scenarios with greater installed capacities approach levels that are similar in the magnitude by which the atmosphere supplies kinetic energy to the wind farm region. As these yield reduction effects relate to the dynamics of the atmosphere, **technological advances in the turbines** are unlikely to be able to compensate for them, although one can minimize the detrimental effects by specific planning of wind farm layouts within the region.

Recommendations

This study suggests that in order to make better use of offshore wind energy, wind farms should be planned and developed with a **coordinated long-term approach**, considering co-dependency of installed capacity density and areal coverage, for efficient deployment.

Future research should continue to analyse the possible impacts of extensive clusters of large and very large wind farms. It should evaluate the limitations and validate the models used here; it should determine to what extent current practice with engineering models fails to capture the removal of kinetic energy demonstrated in our simulations; it should assess the effects of offshore wind energy use on coastal, onshore wind energy; and it should analyse cross-border effects in neighbouring regions, such as the Netherlands, the United Kingdom, or Denmark.

2 Background: More than wakes

Offshore wind energy is seen increasingly as an important contributor for the transition to a carbon-free sustainable energy system in Germany, and in Europe. A number of recent energy scenarios that aim to reduce German CO₂ emissions to 95 % or more by 2050 envision that offshore wind energy can contribute substantially to this goal.

The scenarios for offshore wind energy (Figure 1) project that the installed capacity of Germany's offshore areas (around 8 GW at the end of 2019)¹ will increase by more than eight times to 45 to 70 GW². Yet, the size of offshore regions that Germany admin-

isters are relatively small. They are located primarily in the North Sea, and in border regions administered by neighbouring countries that also intend to develop offshore wind energy. This raises the question of what will happen to wind energy yields when offshore wind farms are expanded to unprecedented scales.

Research over the past few years has evaluated how much wind energy can be expected when used at a very large scale. While such scenarios are hypothetical, they highlight a critical effect: As more wind turbines use more and more of the kinetic energy of the winds in the atmosphere, wind speeds decline, which results in lower yields. These wind speed reductions are a necessary consequence of the limited ability of the atmosphere to generate motion set by thermodynamics, as has been known for a

- 1 Deutsche WindGuard (2018)
- 2 Acatech et al. (2017), Agora Energiewende (2020), BDI (2018), BMU (2015), MWV (2018), Stiftung Offshore (2017)

Installed offshore wind capacity for Germany's 95% climate target scenarios in GW

Figure 1



Acatech et al. (2017), Agora Energiewende (2020), BDI (2018), BMU (2015), MWV (2018), Stiftung Offshore (2017)

while now³. It limits the supply rate of kinetic energy to the near-surface atmosphere at a global average of about 1 W m^{-2} of surface area. Although the supply rate of kinetic energy to the near-surface atmosphere varies from area to area, if wind energy use comes close to the supply rate at large scales, wind speeds necessarily decline. If these wind speed reductions are not taken into account in large-scale wind energy potentials, as is common practice, estimates of large-scale wind energy potential are too high and become inconsistent with the limited ability of the atmosphere to generate kinetic energy⁴. The main

3 Lorenz (1955), Gustavson (1979), Kleidon (2010), Miller et al. (2011)

4 Gans et al. (2012), Miller and Kleidon (2016)

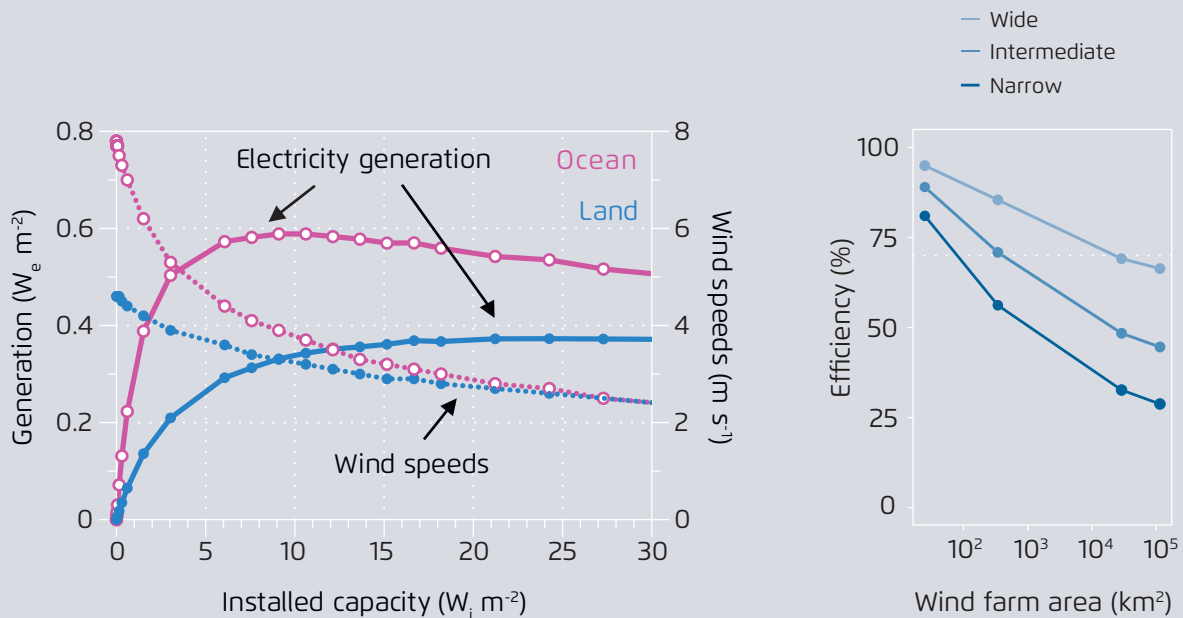
purpose of this report is to evaluate this critical effect on wind energy yields in the scenarios for the German energy transition.

This interplay between larger wind energy use and lower wind speeds is clearly shown by the idealized climate model simulations of Miller and Kleidon⁵ (Figure 2 left). Considering wind turbines installed over the whole planet at different installed capacities, they showed that more wind energy use resulted in lower wind speeds near the surface, which disproportionately lowered the yields of wind turbines since kinetic energy flux depends on wind speed to the power of 3. A reduction of wind speeds by 10%, for

5 Miller and Kleidon (2016)

Recent modelling results suggest that yields decline when wind energy is used at large scales

Figure 2



Left: Simulated electricity generation and mean wind speeds in idealized scenarios of complete coverage of the world with wind turbines of different installed capacities. The maximum generation results from reduced wind speeds at higher installed capacities. (Note that the maximum over land is broader than over the ocean and is reached at a higher installed capacity of $25 \text{ W}_i \text{ m}^{-2}$.)

Right: Simulated drop in efficiency, defined as the capacity factor of a wind farm relative to an isolated turbine, with a greater wind farm area in an idealized scenario of offshore wind energy in the North Sea.

Left: Miller and Kleidon (2016); right: Volker et al. (2017)

example, reduces the kinetic energy flux to $(90\%)^3 = 73\%$, representing a reduction by 27%. What this research suggests is that when wind energy is used at larger scales, the efficiency of wind turbines is reduced due to atmospheric effects, resulting in lower capacity factors and fewer full-load hours. Yet, the simulations considered idealised cases and the results are not specific enough to be used for practical yield estimates in energy scenarios.

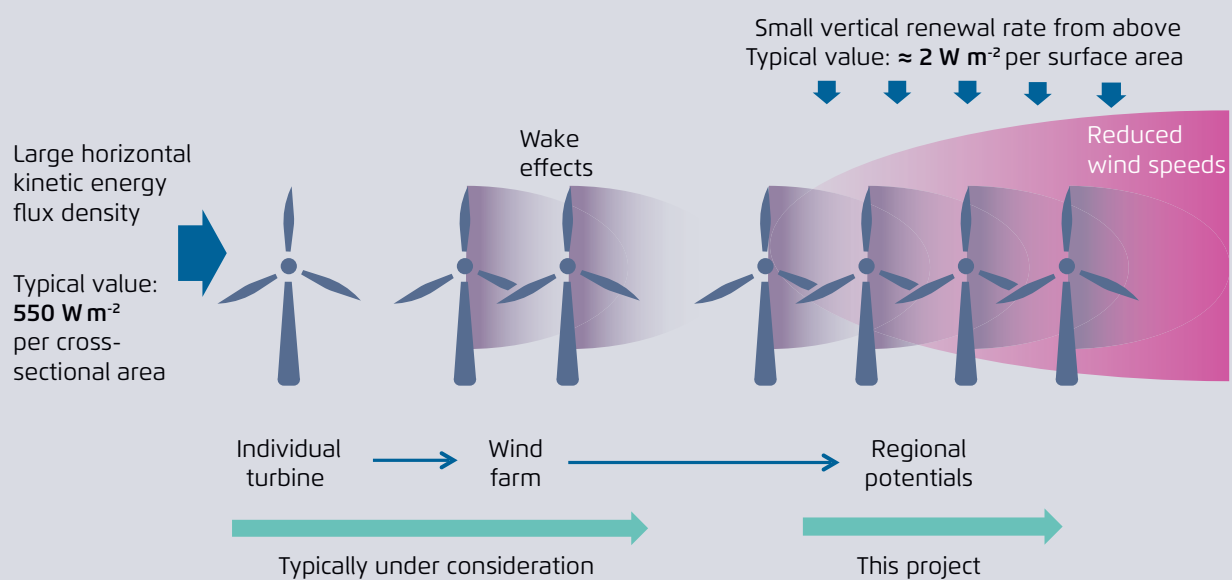
Lower yields when wind energy is used at larger scales were also reported by Volker and colleagues⁶ for a set of hypothetical wind farms of different sizes located in the North Sea (Figure 2 right). They consid-

6 Volker et al. (2017)

ered a number of wind farms of different installed capacity and turbine spacing and evaluated the effect of size. The larger the wind farms were that they considered, the lower the yields, or efficiency, of the turbines compared with the yield of an isolated wind turbine without wake effects. Current wind farms in the North Sea are typically less than 100 km², which results in a fairly small reduction in efficiency. However, when the size is expanded by a factor of ten, as expected in the energy scenarios for 2050, these simulations suggest that efficiency will decline by more than 30%. While turbine technology is likely to develop in the next thirty years, the cause for this reduced efficiency in the simulations is not the technology but the limited ability of the atmosphere to replenish the kinetic energy of the wind farm

The yields of many wind turbines decline by different factors relative to an individual turbine

Figure 3



In a wind farm (middle), wake effects (indicated by the purple shade) of turbines reduce yields of turbines located downwind. At regional scales (right), the effect of turbines of removing kinetic energy from the atmosphere (indicated by pink shade) lowers wind speeds and yields in downwind regions. The values shown in the figure are based on typical values for the annual means for the North Sea, but the actual values show large variations due to varying wind conditions. Note that the magnitude of the vertical renewal rate is limited by the comparatively low generation rate of kinetic energy by the atmosphere, which is set by thermodynamics.

region. This research suggests that as offshore wind energy expands in scale, one would expect that yields decrease due to atmospheric effects. In this study we will evaluate whether this suggestion holds when considering large installed capacities in the North Sea as well as substantially larger wind turbines with altered power and thrust curves.

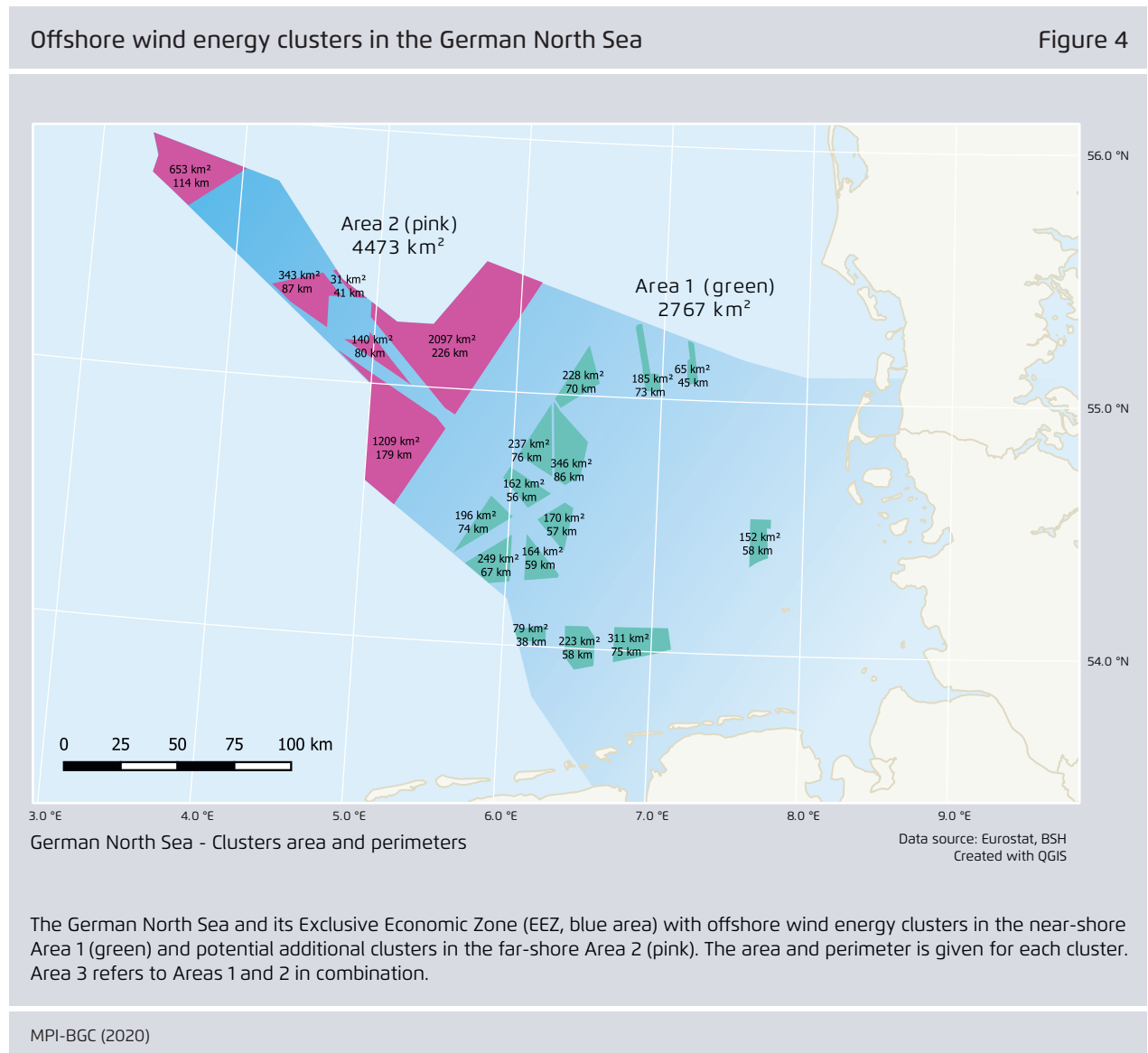
Current energy scenarios typically assume an increase in turbine efficiencies, as expressed by the capacity factor or full-load hours, due to technological developments. The goal here is to evaluate the relevance of atmospheric effects in reducing yields in realistic scenarios of offshore wind energy development in the North Sea using two methods that differ in their complexity. The focus is to evaluate yields that go beyond the typical wake effects considered for wind farms (Figure 3).

We distinguish between the wake effect of individual turbines that reduces the yield of downwind turbines from the kinetic energy removal effect that all turbines cause, resulting in reduced wind speeds and the yield of wind turbines in the region. Wake effects occur behind the wind turbine rotors and the depleted winds are replenished by the surrounding flow. An incomplete replenishment results in a reduced yield of downwind turbines. This effect is well studied and regularly included in yield estimates for wind farms, though it is assumed that the surrounding flow is not affected. Our focus here is to include this effect on the surrounding flow and thereby calculate the overall reduction of kinetic energy of the regional air flow in regional scenarios of offshore wind energy. This study considers the more comprehensive impact of wake effects, which includes the impact on air flow at larger scales.

3 Goals and offshore wind expansion scenarios

This project evaluates a set of offshore scenarios with total installed capacities of offshore wind power covering the range that is considered in German energy scenarios for 2050. We focus these scenarios on the German section of the Exclusive Economic Zone (EEZ) of the North Sea (Figure 4), as it contains

the majority of regions suitable for offshore wind energy in Germany. In the scenarios, we use the characteristics of a hypothetical 12 MW turbine (Figure 5), which we then use to develop different scenarios (Table 2).



3.1 Suitable areas for offshore wind energy

We considered two areas suitable for offshore wind energy generation in the North Sea (Figure 4), a near-shore Area 1 and a far-shore Area 2. These areas, which are separated by a major shipping route, were determined by excluding other maritime uses following the procedure recommended by the Federal Maritime and Hydrographic Agency (BSH). We excluded shipping routes, areas next to cables and pipelines, as well as areas for nature protection, research, and military purposes⁷.

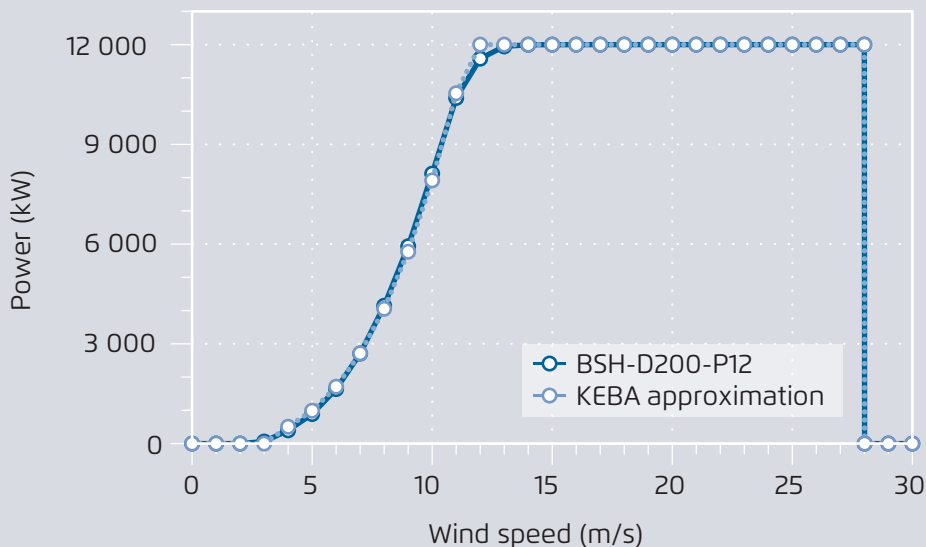
⁷ The spatial data of the German maritime area, military areas, pipeline areas and wind park clusters in area 1 were downloaded from the geodata portal of the German service of maritime navigation and the seas (BSH, <https://www.geoseaportal.de>). The coordinates of shipping routes and research areas were extracted from the regional planning document (https://www.bsh.de/DE/THEMEN/Offshore/Meeresraumplanung/Nationale_

The resulting clusters in Area 1 amount to a total windfarm coverage area of 2,767 km², while the clusters in Area 2 amount to a total windfarm coverage area of 4,473 km². Area 3 combines Areas 1 and 2, resulting in a total windfarm coverage area of 7,240 km². Note that current expansion plans for offshore wind energy in Germany only consider clusters in Area 1. Also note that these areas only refer to places where wind turbines are being installed. These areas are necessary to convert a given density of installed capacity into an actual number of wind turbines and a total installed capacity. For the estimation of wind energy yields, the areas between windfarms are also considered because the wakes from upwind windfarms recover in these areas, at least in part.

Raumplanung/_Anlagen/Downloads/Raumordnungsplan_Textteil_Nordsee.pdf). Nature protection areas were obtained from the German Federal Agency of Nature Conservation.

Power curve of a hypothetical 12 MW wind turbine in the offshore wind energy scenarios

Figure 5



MPI-BGC (2020)

3.2 Assumed turbine technology

We used the specifications of a hypothetical 12 MW wind turbine, "BSH-200-P12", obtained from Deutsche WindGuard on behalf of BSH. The turbine is assumed to have a hub height of 140 m, a rotor-swept diameter of 200 m, a cut-in velocity of 3 m/s, a rated velocity of about 12 m/s, and a cut-out velocity of 28 m/s. The power curve of this turbine is shown in Figure 5.

When operated in isolation, this turbine would be expected to yield about 4,410 – 4,930 hours of full-load or about 53 to 59 GWh/year given the typical wind conditions of the region (Figure 6). The range of hours of full-load comes from the different wind forcing data used for the evaluations here.

3.3 Definition of scenarios

We developed a range of scenarios using different densities of installed capacity, ranging from 5 MW/km² to 20 MW/km² for Area 1, Area 2 and Area 3 (Table 2). This yields a range of total installed capacity from 13.8 GW to 144.8 GW, corresponding to a total of 1,153 to 12,067 GW turbines with 12 MW each. The abbreviations for these scenarios are listed in the first column of Table 2 and are composed of the installed capacity density (5 to 20 MW km⁻²) followed by the areas populated by the turbines (A1, A2, A3).

Note that the current expansion plans for offshore wind energy only consider Area 1, not Area 2 or Area 3. The associated scenarios 5A1 to 20A1 repre-

List of considered scenarios with different capacity densities and areas of installations.

Table 2

| Scenario | Capacity density (MW/km ²) | Area used | Installed capacity (GW) | Number of 12 MW turbines |
|----------|--|-----------|-------------------------|--------------------------|
| 5A1 | 5.0 | A1 | 13.8 | 1,153 |
| 5A2 | 5.0 | A2 | 22.4 | 1,864 |
| 5A3 | 5.0 | A1 + A2 | 36.2 | 3,017 |
| 7.5A1 | 7.5 | A1 | 20.8 | 1,729 |
| 7.5A2 | 7.5 | A2 | 33.5 | 2,796 |
| 7.5A3 | 7.5 | A1 + A2 | 54.3 | 4,525 |
| 10A1 | 10.0 | A1 | 27.7 | 2,306 |
| 10A2 | 10.0 | A2 | 44.7 | 3,728 |
| 10A3 | 10.0 | A1 + A2 | 72.4 | 6,033 |
| 12.5A1 | 12.5 | A1 | 34.6 | 2,882 |
| 12.5A2 | 12.5 | A2 | 55.9 | 4,659 |
| 12.5A3 | 12.5 | A1 + A2 | 90.5 | 7,542 |
| 20A1 | 20.0 | A1 | 55.3 | 4,612 |
| 20A2 | 20.0 | A2 | 89.5 | 7,455 |
| 20A3 | 20.0 | A1 + A2 | 144.8 | 12,067 |

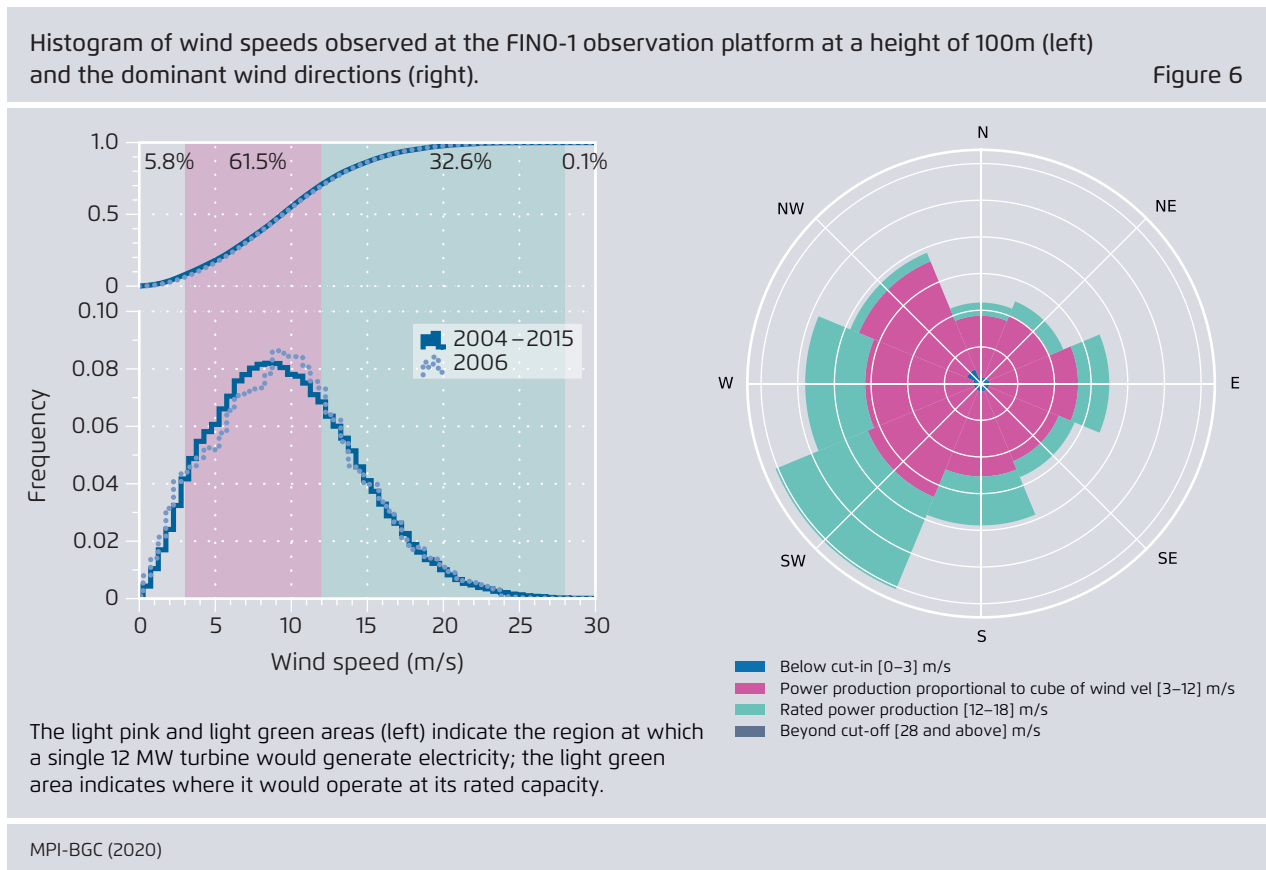
DTU and MPI-BGC (2020)

sent a range of 13.8 to 55.3 GW of installed capacity, and thus do not cover the complete range of the scenarios shown in Figure 1 for the year 2050. The scenarios 12.5A3, 20A2 and 20A3 take into account installed capacities that exceed the total installed capacity that is currently considered in energy scenarios for the year 2050. They are included here to perform the evaluation with a consistent setup.

3.4 Typical wind climatology in the region

As background, the wind climatology of the region is shown in Figure 6, using observations at a 100 m height from the FINO-1 observation platform in the North Sea. It shows the frequency distribution of wind speeds (Figure 6 left) and directions (Figure 6 right), and groups these into different wind regimes: wind speeds < 3 m/s (no power generated by the

turbine), 3 – 12 m/s (generation depends on wind speed), 12 – 28 m/s (generation at turbine’s capacity) and above (no generation). These wind regimes represent 5.8 %, 61.5 %, 32.6 %, and 0.1 % of the time, respectively. Under these wind conditions, one would expect a single turbine to have 4,928 hours of full-load per year, yielding a capacity factor of 56.3 % and generated electricity of 59.1 GWh per year. This estimate represents an ideal reference case without the reduction effects due to wakes and kinetic energy removal.



4 Methods

4.1 Overview

We use two methods, KEBA and WRF, to estimate wind speed reductions using descriptions of the atmospheric flow surrounding the wind farm regions. While these effects on wind speed have not been tested against observations, partly due to the fact that such large wind farms do not yet exist, there are good reasons to think that these estimations are realistic. While the KEBA method is based on physical first principles, the WRF method is based on physical descriptions of atmospheric flow. The latter is commonly used to simulate realistic regional weather and climate.

In addition to simulating reduced wind speeds, we obtained wind turbine yields for the scenarios listed in Table 2. The two methods differ substantially in complexity, with KEBA being simple and fast, and WRF being highly detailed and requiring a computer cluster to perform the simulations. Because of the computational intensity of the WRF method, only some of the scenarios have been evaluated.

The main features of the two methods are summarized in Table 3.

Summary of the two methods used to simulate the effects of wind speed reductions on energy yields for the offshore scenarios.

Table 3

| | KEBA Method | WRF Method |
|--------------------|--|---|
| Simulations run by | MPI: Max-Planck-Institute for Biogeochemistry | DTU: Technical University of Denmark, Department of Wind Energy |
| Meaning of acronym | Kinetic Energy Budget of the Atmosphere | Weather Research and Forecast model |
| Type of method | Box model implemented in a spreadsheet | Numerical model used for weather forecasting simulating the three-dimensional atmospheric flow on a high resolution grid with dimensions of 2 km. Model code executed on a cluster computer |
| Input data | Time series of observed wind speeds, taken from the FINO-1 observation platform for the years 2004-2015 ⁸ | Time series of three dimensional meteorological fields from the European Centre for Medium-Range Weather Forecasts (ECMWF) |
| Output | Time series of total yield and wind speed reduction | Time series of three-dimensional fields of meteorological variables and yields of different wind farm clusters |

⁸ The evaluations with FINO-1 data were performed using only the first part of the time series, during which the measuring site is unlikely to be influenced by surrounding wind farms. However, no notable difference in the results could be found.

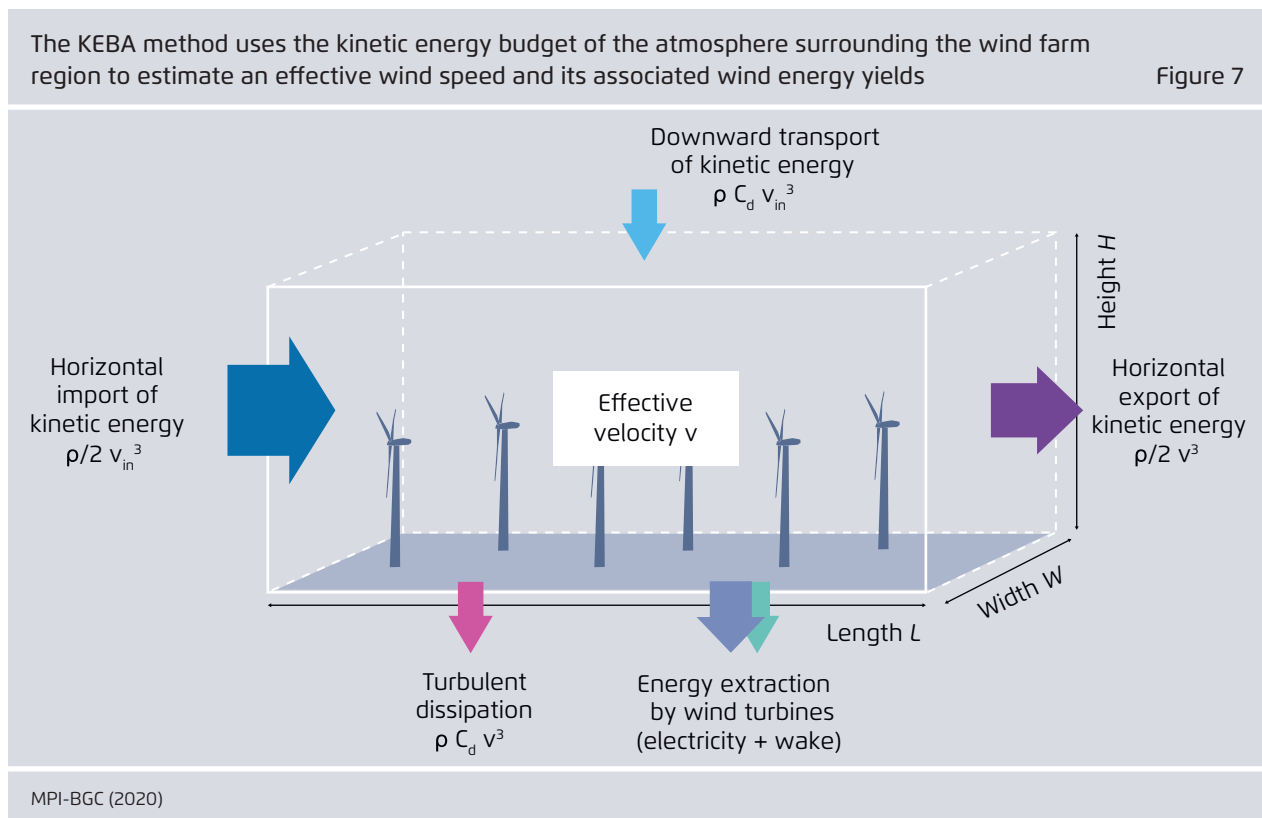
4.2 KEBA: Kinetic Energy Budget of the Atmosphere

The KEBA method uses the kinetic energy budget of the atmosphere surrounding the wind farms to diagnose wind speed reductions and estimates energy yields (Figure 7).

To set up this budget, a rectangular box is considered with dimensions representative of the wind farm region. The dimensions of the box are given by an effective cross-sectional width W , a height H , and a downwind length L (as labelled in Figure 7). The height H is taken to be 700 m, representative of the typical height of the well-mixed maritime boundary layer. For the drag coefficient C_d , a typical value of 0.001 was used. These two parameters somewhat affect the estimates of the KEBA method and may change depending on the particular region or season, yet the sensitivity of the results is relatively insensitive to reasonable variations of these two parameters.

A full exploration of such sensitivities is beyond the scope of the present study. Note that the use of the boundary layer height H means that an increase of mixing because of the wind turbines is accounted for as long as these effects remain within the boundary layer. Different configurations for the width and downwind length were used, as described below.

The kinetic energy budget of this box consists of fluxes that supply and remove kinetic energy. The supply of kinetic energy comes from the influx through the upwind cross-sectional area, which is proportional to air density ρ and wind speed cubed ($\rho/2 v_{in}^3$; dark blue arrow in Figure 7), and the vertical mixing from above (light blue arrow). This latter flux is assumed to be similar to the natural, frictional dissipation, which is characterized by the so-called drag formulation of shear stress ($\rho C_d v_{in}^3$) with a drag coefficient C_d , which also depends on wind speed cubed, but has a much smaller magnitude.



Kinetic energy is removed from the box due to the energy removed by the wind turbines (blue-grey arrow in Figure 7), to wake turbulence (turquoise arrow), to frictional dissipation at the surface (pink arrow), and to the outflow through the downwind cross-sectional area of the box (purple arrow). The energy removed by the turbines is described by the power curve (Figure 5) and the number of wind turbines of the scenario. Wake turbulence is taken to be 1/2 of the removed energy by the turbines⁹. Surface frictional dissipation and outflow use the same formulations as the influxes of kinetic energy, except that the employed effective wind velocity is smaller than the velocity of the inflow.

The terms of the kinetic energy budget yield a formula that describes the effective velocity of air flow within the box from which the yield is estimated. It requires the specification of the box dimensions, the drag coefficient, the power curve as well as the number of turbines of the scenario together with a time series of observed wind speeds. The chosen parameter values as well as the dimensions used for the scenarios are specified in the Appendix. The observations from FINO-1 (Figure 6) were used to provide the input wind speeds.

We considered different configurations for the width and downwind length, resulting in a set of four KEBA estimates. The first case ("reference") assumes a simple layout in which all wind turbines are located in a hypothetical square representative of the total cluster area (as shown in Figure 4). The horizontal dimensions of this square are 52.6 km for Area 1, 66.9 km for Area 2, and 85.1 km for Area 3. The second case ("directions") considers the specific dimensions of the clusters as well as the wind directions in the estimate, with wind directions being partitioned into 8 classes (as shown in Figure 6 on the right).

Two other cases are considered that demonstrate the importance of these dimensions. In a third case ("widest"), the widest width of the cross-sectional area of the clusters for the main wind direction from the southwest is used, while the fourth case ("longest") considers the longest downwind length in the main wind direction.

Cases 1, 3, and 4 are evaluated with an Excel spreadsheet, while Case 2 ("directions") was implemented in a relatively simple computer programme. Cases 1 and 2 aimed to provide reasonable estimates of wind energy yields, while Cases 3 and 4 ("widest" and "longest") are hypothetical and have the purpose of illustrating the importance of the dimensions and layout of wind farms.

4.3 WRF: Weather Research and Forecasting Model

Mesoscale modelling

The central element of the methodology employed by DTU is the mesoscale model known as Weather Research and Forecasting Model (WRF¹⁰). This model provides numerical weather prediction of the kind that is used by weather forecasting centres and researchers all over the world, including National Centers for Environmental Prediction (NCEP) in the USA. Mesoscale modelling refers to scales of motions in the atmosphere down to approximately 1 km in size. A mesoscale model is able to capture the development of weather systems, such as low pressure systems, and the development and passage of frontal systems. Mesoscale modelling attempts to capture the dynamics of motions of the atmosphere and thermodynamics of the atmosphere. Some processes of the atmosphere are resolved by the model grid, whereas other processes need to be parameterized because either they are not resolved by the grid, or because the model does not represent the physics of a particular process. Parameterizations may include convec-

9 Corten (2001)

10 Skamarock et al. (2008)

tion, turbulence, radiative transfer, and air surface interaction, among other processes.

The National Center for Atmospheric Research (NCAR) in the USA coordinates workshops and tutorials for a community of around 50,000 users worldwide.

Representing wind farms in mesoscale models

The WRF mesoscale model cannot resolve the influence of wind turbines directly due to the difference in scale between model resolution and the scale of the turbines. Therefore, the influence of wind turbines needs to be parameterized in the mesoscale model. Two main parameterizations have been developed for this purpose in the WRF model, the Explicit Wake Parameterization (hereafter referred to as EWP¹¹) and the Wind Farm Parameterization (hereafter referred to as WFP¹²). For full details of the parameterizations, see the respective publications. In the following paragraphs, the essential elements and comparisons of the methods are described.

The Explicit Wake Parameterization (EWP) works by imposing a turbine thrust in the opposite direction to the wind direction, causing a deceleration in the flow of air. Any mesoscale grid box with wind turbines present will impose this thrust on the flow. The magnitude of the thrust is a function of the number of turbines and the wind speed. The thrust is centred around the hub height and distributed vertically above and below the rotor diameter in order to represent a vertical expansion of the turbine wake occurring in the mesoscale grid box. This is one of the main differences in the EWP method and the WFP method. In WFP the distribution of the thrust is defined by the rotor intersection area at different heights. Another important difference is that the WFP method, while not modelling wake farm expansion within a grid box, adds turbulent kinetic energy in the mesoscale model to trigger greater mixing via

the turbulence parameterization within WRF. The EWP method leaves the generation of turbulent kinetic energy and increased mixing to the turbulence parameterization model in WRF.

The two methods were compared at the Horn Rev wind farm and checked against wind measurement data¹³. Filtering the measurement data to focus on 10 m/s westerly inflow in neutral conditions, a study found that the EWP and WFP methods had a similar maximum deficit on the downwind side of the Horn Rev wind farm (0.1% difference), but that the wind speed dropped initially more rapidly in the WFP scheme. The wake recovery was more rapid in the WFP method. At 2 km and 6 km downwind, the wind speed was approximately 5% and 3% higher, respectively, than measurements, while the EWP method was closer to measurement. As a consequence of the difference in wake recovery rates, the length of the wakes is longer in EWP (at 21 km) than in WFP (at 11 km) - measured by the distance where the wind speed recovers to within 7.5% of the undisturbed flow.

One study found that within large wind farms winds tended to be lower in WFP than in EWP¹⁴. A very recent study¹⁵ has used the EWP and WFP parameterizations to investigate wakes at the Sandbank and DanTysk windfarms in the North Sea, and validated them against mean wind farm wind speed and wind farm power generation data from these wind farms for 2018. The EWP scheme yielded a bias of 0.23 m/s and 0.18 m/s at Sandbank and DanTysk, respectively, compared with WFP, which yielded a bias of -0.14 m/s and -0.21 m/s for the two wind farms. Similarly, the estimated mean power generation is overestimated using EWP by 18 GW (out of a rated power of 288 GW) and 12 GW (out of a rated power of 288 GW) for the two wind farms, and underestimated using WFP by 4 GW and 7 GW, respectively. Alto-

11 Volker et al. (2015)

12 Fitch et al. (2012)

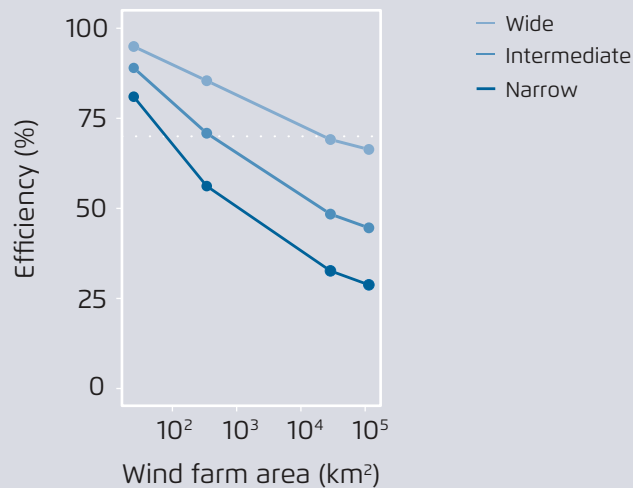
13 Volker et al. (2015)

14 Volker et al. (2017)

15 Langor (2019)

Wind farm efficiency plotting against wind farm size for 3 different installed capacity densities

Figure 8



Capacity densities: 2.8 MW/km² (light blue), 6.4 MW/km² (medium blue), and 11.3 MW/km² (dark blue). The wind climate is from Horn Rev in the North Sea.

Volker et al. (2017)

gether, the net effect of these differences in wind farm parametrizations depend on the influence of intra-farm wake losses and inter-farm wakes losses, i.e. the losses caused by wakes developed by a wind farm's own turbines and losses caused by wakes from a neighbouring wind farm.

Examples of previous work using this kind of modelling

Volker et al. (2017) is an example of a study that uses mesoscale wind farm parameterizations and investigates wind farm production via modelling different size wind farms, with different installed capacity densities subject to different wind climates. Defining the efficiency of a wind farm as the ratio of production accounting for wake losses to production with no wake losses, Figure 8 shows how the efficiency drops as wind farm size increases. Very large wind farms and high installed capacity densities exacerbate the drop in efficiency.

Nevertheless, even when accounting for wake losses¹⁶, reasonable choices exist for numerous large wind farms that can meet electricity demand in the USA or the European Union before low efficiencies occur.

Mesoscale modelling including wind farm wake effects was performed for an existing wind farm cluster in the USA¹⁷. The study used mesoscale modelling to estimate generation losses at one wind farm due to the wakes of an upwind farm. An example flow situation is given that exhibits a power generation loss of one sixth of the effected wind farm capacity (45 MW out of 270 MW).

Specific WRF set-up

The WRF version used is WRF 3.8.1. The WRF model domain consists of 3 one-way nested domains with a resolution of 18 km (outermost domain 1), 6km, and

¹⁶ Badger and Volker (2017)

¹⁷ Lundquist et al. (2019)

2 km resolution (innermost domain). Figure 9 shows the computational domains used with focus on the coverage of the southeast part of the North Sea. The results from the highest resolution innermost domain were then analysed. The forcing data for the lateral boundary conditions come from the ECMWFs ERA5 Reanalysis dataset¹⁸. The sea surface temperatures come from the Operational Sea Surface Temperature and Sea Ice Analysis (OSTIA¹⁹). A full calendar year is

18 C3S (2017)

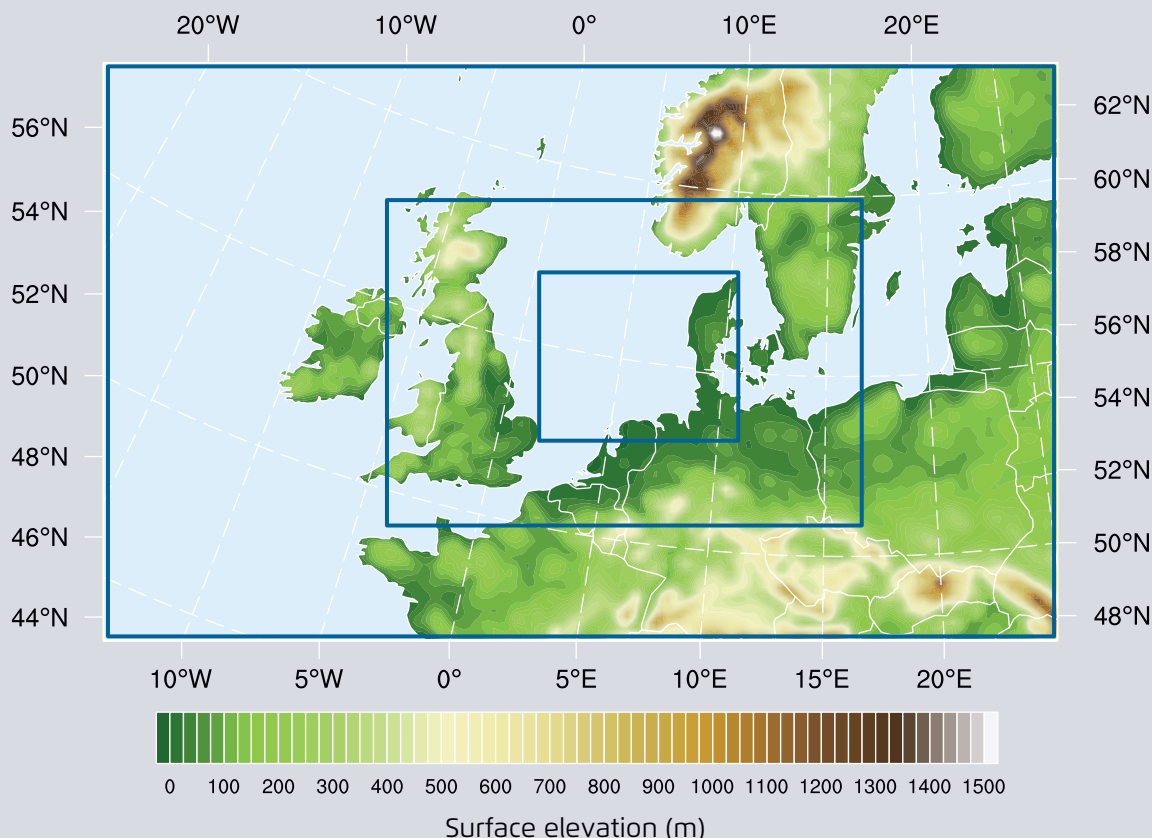
19 Donlon et al. (2012)

simulated for each scenario. It is split up into blocks of 11 days, whereby the past 24 hours of a block overlap with the first 24 hours of the following block. In each block, the first 24 hours is discarded due to model spin-up. For the sake of method transparency, the "namelist" for the WRF model simulations is given in the Appendix.

The wind farms are represented in the mesoscale model by projecting the extent of future wind farm areas onto the model grid boxes. Figure 10 shows the wind farm locations within the innermost computa-

Map showing the nested WRF calculation domains used for this study

Figure 9



There are three domains: the outer domain comprising the whole displayed map; the intermediate domain comprising much of the British Isles and Northern Germany and southern Scandinavia; and the inner domain, comprising the south eastern North Sea and parts of Northern Germany and Western Denmark.

DTU (2020)

tional domain on the 2 km grid boxes. The individual extent of each wind farm area is resolved so that even gaps between the wind farms areas can be seen.

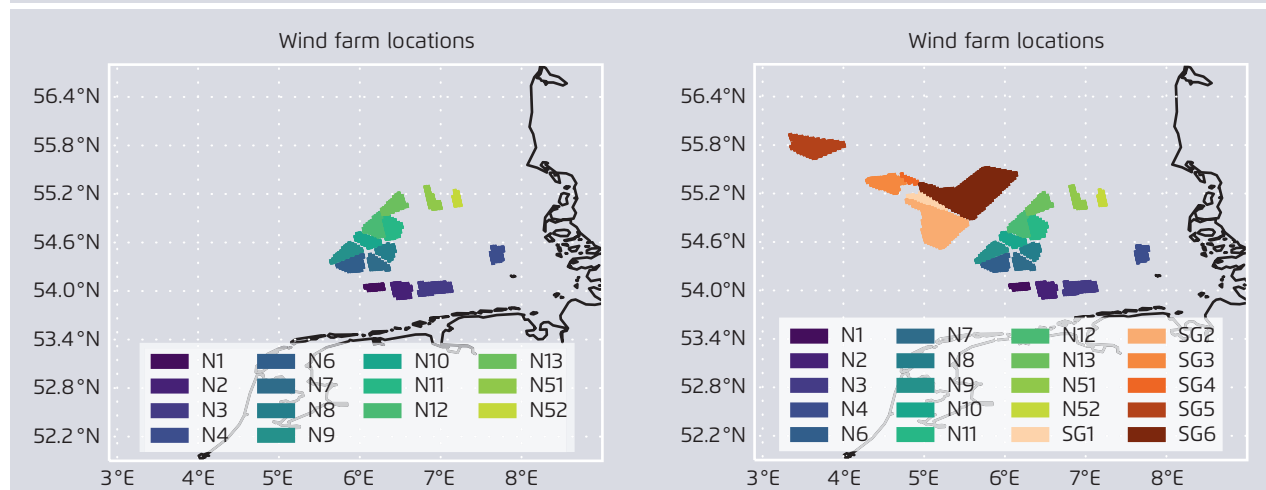
Selection of the WRF simulation year

The foundation for the selection of a climatological representative year was based on tabulated data from the Central European (CE) domain, which was created within the New European Wind Atlas project. The available data range at the point of determination were full-year runs from 2001 to 2017. The different years were compared in three different categories important for wind farm wakes: wind speed distribution, wind direction distribution, and atmospheric stability. The following analysis was then performed for 10 randomly selected points in the southern North Sea area. First, a climatological representative year based on the distribution average of all years between 2001 and 2017 was constructed for each parameter at the given location and compared with the distribution of a particular year at that location. The earth mover's

distance was used as an objective measure for the similarity of the distributions. Then, the different years were ranked for each parameter at each location. As a final step, the year with the highest ranking of 10 locations was chosen. The different parameters were set to have equal weight in the decision process. The outcome of the representative year analysis was 2006.

Maps showing the representation of wind farms in inner area A1 (left) and in the inner and outer areas A3 (right).

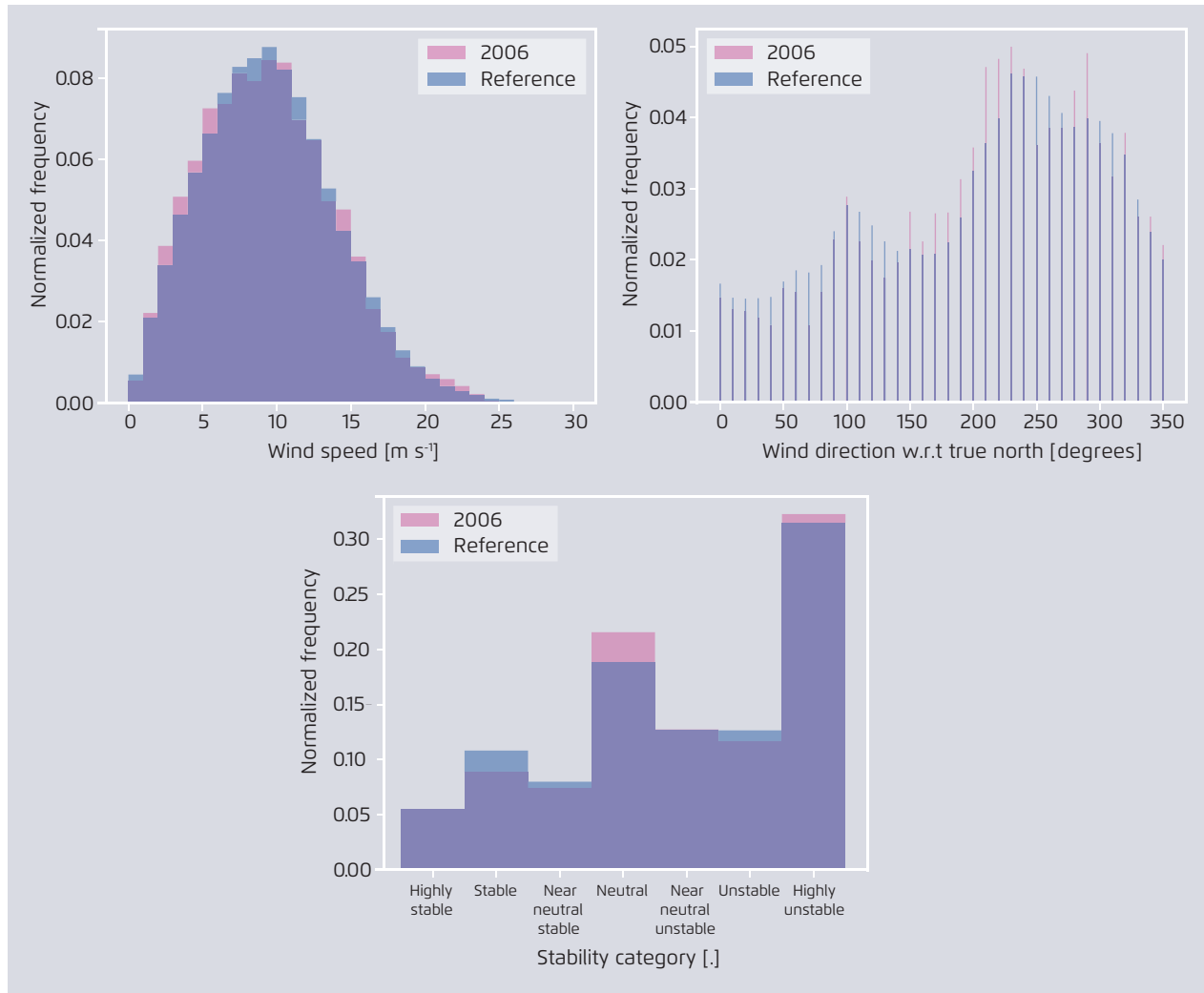
Figure 10



These two representations of wind farms are used in the mesoscale simulations and in the reference simulation without any wind farms. Each plotted coloured point represents a mesoscale grid box in which wind turbines are present.

Comparison of distributions of wind speed (top left), wind direction (top right), and boundary layer stability (bottom) for the simulation year (2006) and the reference period

Figure 11



DTU (2020)

5 Results

5.1 Overview

The two methods to estimate the effect of wind speed reductions on offshore wind energy yields provide rather different forms of output. The KEBA method, implemented in a spreadsheet, provides highly abstracted and aggregated outcomes for the scenarios, while the WRF simulations provide highly detailed fields of output that can be used to estimate yields within each of the clusters in the areas. In the following, the results of each method are described individually and are then compared to each other.

5.2 KEBA results

The KEBA estimates for the different scenarios are summarized in Table 4 and shown in Figures 12 and 13 in terms of estimated annual yields and turbine efficiencies (i.e., estimated yield relative to an isolated turbine). These estimates are compared with the yields of single, isolated turbines (columns "Isolated" in Table 4), that is to say, the case without any wake or kinetic energy removal effects.

The estimates by KEBA are generally lower due to the reduced wind speeds. This reduction effect becomes more important in the scenarios with a higher

Summary of the yield estimates in the KEBA approach for the different scenarios

Table 4

| Scenario | KEBA Cases | | | | | | | | | |
|----------|------------|-----------|-------------|-----------|--------------|-----------|------------|-----------|------------|-----------|
| | "Isolated" | | "Reference" | | "Directions" | | "Widest" | | "Longest" | |
| | Yield (GW) | FLH (h/a) | Yield (GW) | FLH (h/a) | Yield (GW) | FLH (h/a) | Yield (GW) | FLH (h/a) | Yield (GW) | FLH (h/a) |
| 5A1 | 7.8 | 4,928 | 6.4 | 4,065 | 6.0 | 3,808 | 7.1 | 4,499 | 5.3 | 3,358 |
| 5A2 | 12.6 | 4,928 | 10.0 | 3,913 | 9.0 | 3,545 | 11.1 | 4,351 | 8.9 | 3,488 |
| 5A3 | 20.4 | 4,928 | 15.4 | 3,729 | 15.0 | 3,623 | 18.3 | 4,431 | 13.7 | 3,318 |
| 7.5A1 | 11.7 | 4,928 | 8.8 | 3,713 | 8.3 | 3,520 | 10.2 | 4,309 | 6.7 | 2,830 |
| 7.5A2 | 18.9 | 4,928 | 13.5 | 3,530 | 12.3 | 3,203 | 15.8 | 4,129 | 11.6 | 3,031 |
| 7.5A3 | 30.5 | 4,928 | 20.5 | 3,309 | 20.3 | 3,280 | 26.1 | 4,213 | 17.6 | 2,841 |
| 10A1 | 15.6 | 4,928 | 10.9 | 3,449 | 10.3 | 3,261 | 13.0 | 4,118 | 7.8 | 2,471 |
| 10A2 | 25.2 | 4,928 | 16.4 | 3,216 | 14.9 | 2,913 | 20.0 | 3,920 | 13.5 | 2,646 |
| 10A3 | 40.7 | 4,928 | 24.5 | 2,966 | 24.8 | 3,002 | 33.1 | 4,008 | 20.4 | 2,470 |
| 12.5A1 | 19.5 | 4,928 | 12.6 | 3,190 | 12.0 | 3,057 | 15.7 | 3,979 | 8.6 | 2,180 |
| 12.5A2 | 31.5 | 4,928 | 18.8 | 2,949 | 17.0 | 2,671 | 23.7 | 3,716 | 15.1 | 2,367 |
| 12.5A3 | 50.9 | 4,928 | 27.7 | 2,683 | 28.5 | 2,762 | 39.5 | 3,826 | 22.4 | 2,170 |
| 20A1 | 31.1 | 4,928 | 16.4 | 2,600 | 16.2 | 2,559 | 22.4 | 3,548 | 10.0 | 1,584 |
| 20A2 | 50.3 | 4,928 | 23.8 | 2,331 | 21.9 | 2,144 | 32.8 | 3,214 | 17.9 | 1,754 |
| 20A3 | 81.5 | 4,928 | 34.2 | 2,070 | 37.0 | 2,237 | 55.5 | 3,360 | 26.1 | 1,580 |

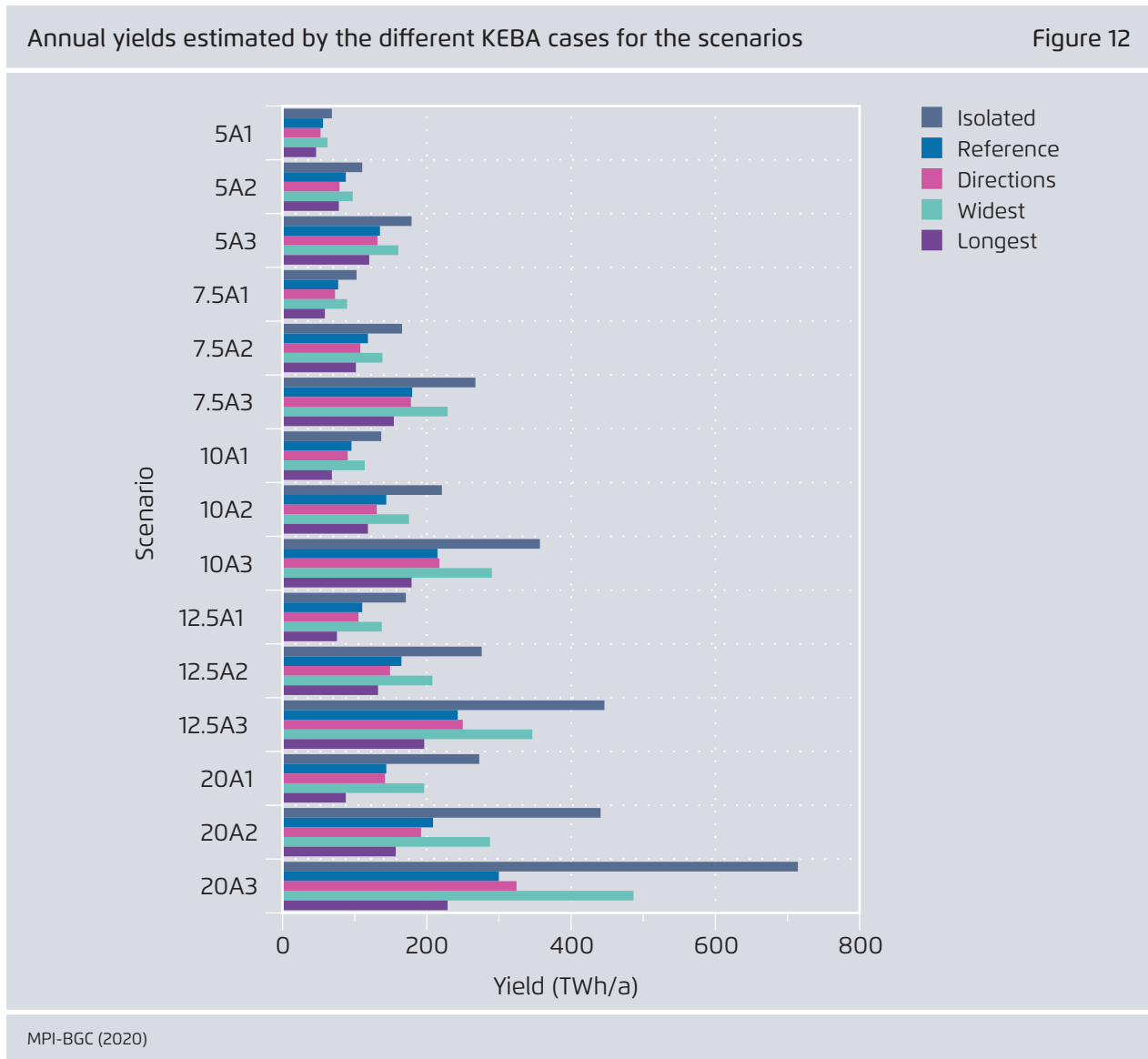
MPI-BGC (2020)

installed capacity. For relatively low installed capacities, as in the scenarios 5A1 to 5A3, KEBA estimates yield reductions by about 18.0 to 26.5% (for cases "Reference" and "Directions"). This reduction increases with greater installed capacities to 47.3 to 58.0% in scenarios 20A1 to 20A3 (Figure 13).

The effects of the layout of the clusters can be seen in the hypothetical cases "Widest" and "Longest". The "Widest" case considers a wider cross-sectional area into which kinetic energy is imported in the wind farm region, so the effects can still occur, but at a

smaller magnitude. As this case uses the dimensions of the dominant wind direction, the results are not representative for the overall yield of all wind farms as it yields estimates that are too high. The "Longest" case considers the longest downwind dimension so the effect of wind speed reductions is enhanced, resulting in lower yields than the "Reference" case.

The estimated change in the wind speed distribution is illustrated for two of the scenarios in Figure 14. It shows the wind speed distribution observed at the FINO-1 station and the estimated reductions in the



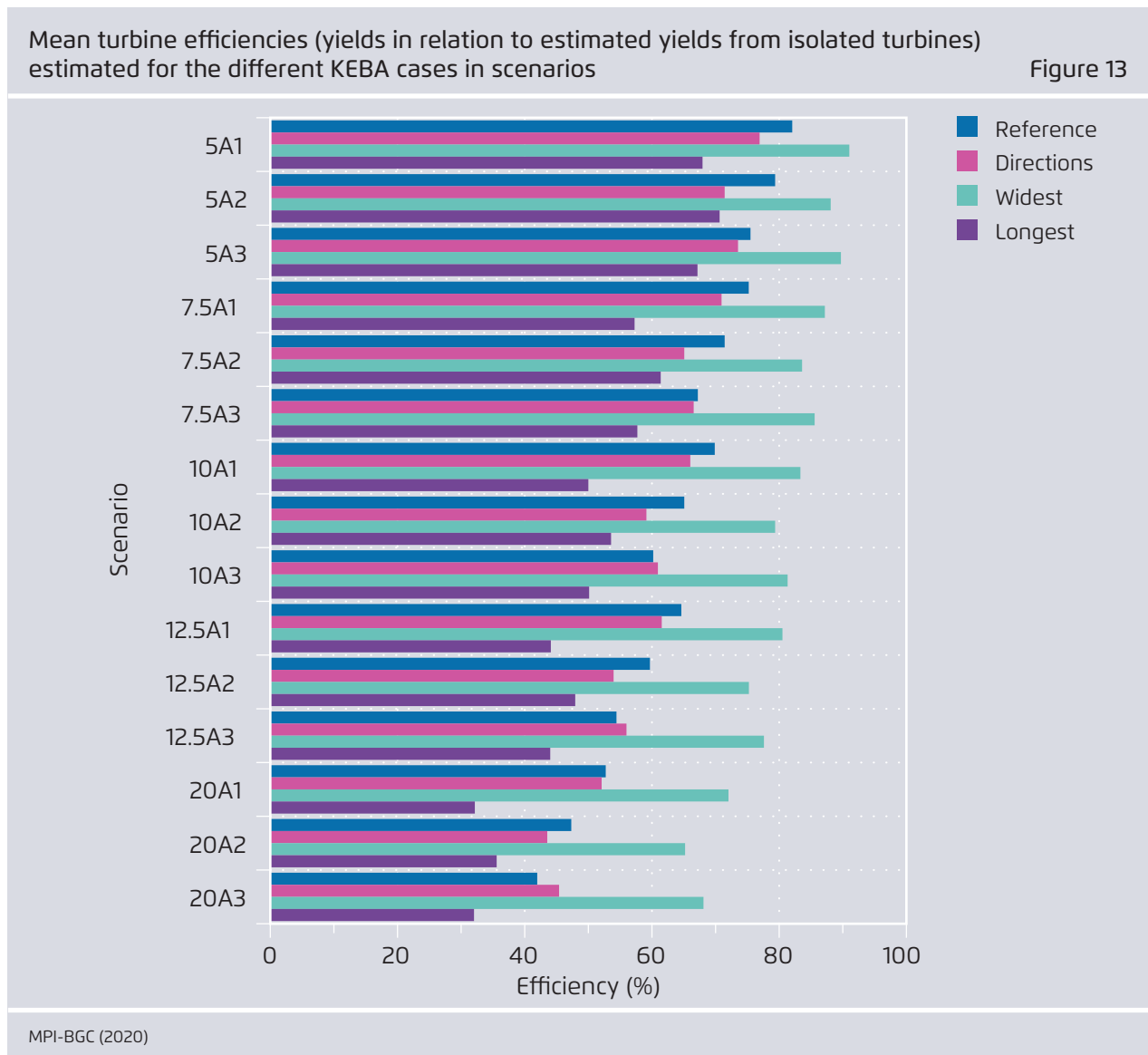
scenarios 5A1 and 20A1. High wind speeds noticeably decrease in frequency, while lower wind speeds below the rated velocity increase, so the distribution results in a shift such that wind turbines are likely to operate more often below their capacity. The strong change in response around the rated velocity of 12 m/s is due to the difference in the functional relationship by which wind turbines remove kinetic energy. Below the rated velocity, wind turbines remove kinetic energy proportional to the kinetic energy flux, while above the rated velocity wind turbines operate at capacity and thus remove a fixed amount. The

spike at 3 m/s in the histograms is due to reaching the cut-in velocity.

As KEBA is based on the budgeting of kinetic energy fluxes, it is instructive to look at how these kinetic energy fluxes change in scenarios of higher installed capacity. Figure 15 shows three selected scenarios, 5A1, 10A1, and 20A1, with installed capacities of about 14 GW, 28 GW, and 55 GW respectively for the KEBA "Reference" case. It shows that in the 5A1 scenario with relatively low installed capacities, wind turbines extract a comparatively small fraction of

Mean turbine efficiencies (yields in relation to estimated yields from isolated turbines) estimated for the different KEBA cases in scenarios

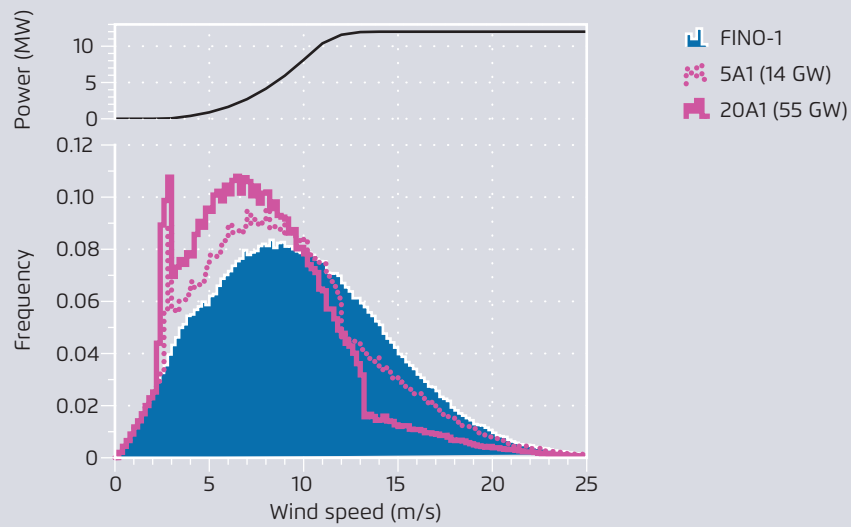
Figure 13



MPI-BGC (2020)

Change in wind speed frequency estimated for different scenarios (bottom) and power curve for the assumed 12 MW turbine (top)

Figure 14



The 5A1 (red dotted line, 14 GW installed capacity) and the 20A1 (red solid line, 55 GW installed capacity) scenarios are compared with the climatology of wind speeds observed at the FINO-1 platform. Also shown for comparison at the top is the power curve for the assumed 12 MW turbine.

MPI-BGC (2020)

Estimated kinetic energy influxes and outflows

Figure 15



Influxes into the region as well as the share that is extracted by wind turbines (grey), that is lost by wake turbulence (turquoise) or surface friction (pink), or that leaves the region downwind (purple). The same colours are used for the arrows in the KEBA schematic diagram in Figure 7.

MPI-BGC (2020)

15% of the kinetic energy that enters the surrounding atmosphere. This fraction increases to 26% in the 10A1 scenario and to 39% in the 20A1 scenario, so that the removal of kinetic energy by the wind turbines makes up an increasing share of the kinetic energy transported to the region. This increasing proportion can explain why wind speeds decrease within the region as installed capacities increase, and why, as a result, the yields decline.

5.3 WRF results

Wind speed of the mesoscale simulations

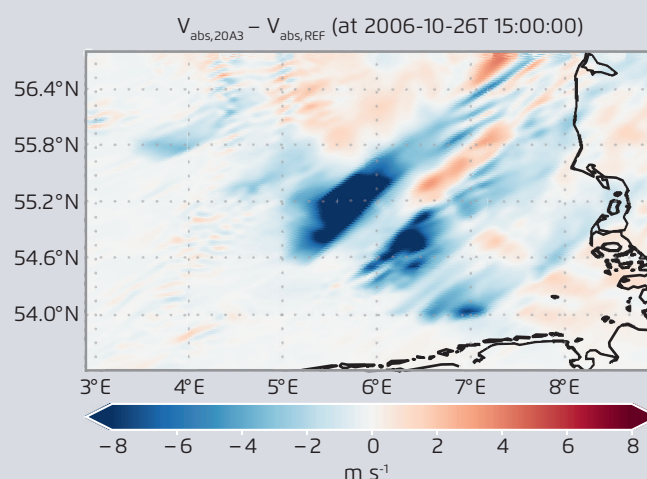
In this section the mesoscale modelling outputs are presented for a single scenario to indicate the behaviour of the wind farm wakes. Figure 16 shows a map of the wind speed difference for the scenario with maximum installed capacity density and number of wind farms shown for a particular time, namely 26 October 2006 at 15:00 GMT, compared with the

reference simulation at the same time. This is given solely as an example to indicate that the wind speed deficit extends to 100 km downwind of the wind farms. It also indicates the complexity of the patterns in the wind speed difference. It produces negative differences, as shown by the wakes, and positive differences, indicating faster speeds than in the reference simulation.

In Figure 17 the total effect on mean wind speed of the wind farms for the entire year is shown for the same scenario. Here the downwind extent of the wakes is less pronounced because given the range of wind directions the wake effect is smeared out by the averaging. Nevertheless, it can be seen that within the wind farms there is a significant reduction in wind speed (> 25% lower) and within 10 km of the wind farms the wind speed decreases markedly (> 10% lower).

Map showing the difference between wind speed at approximately hub height for scenario 20A3 and the reference simulation for 15:00 GMT on 26 October 2006

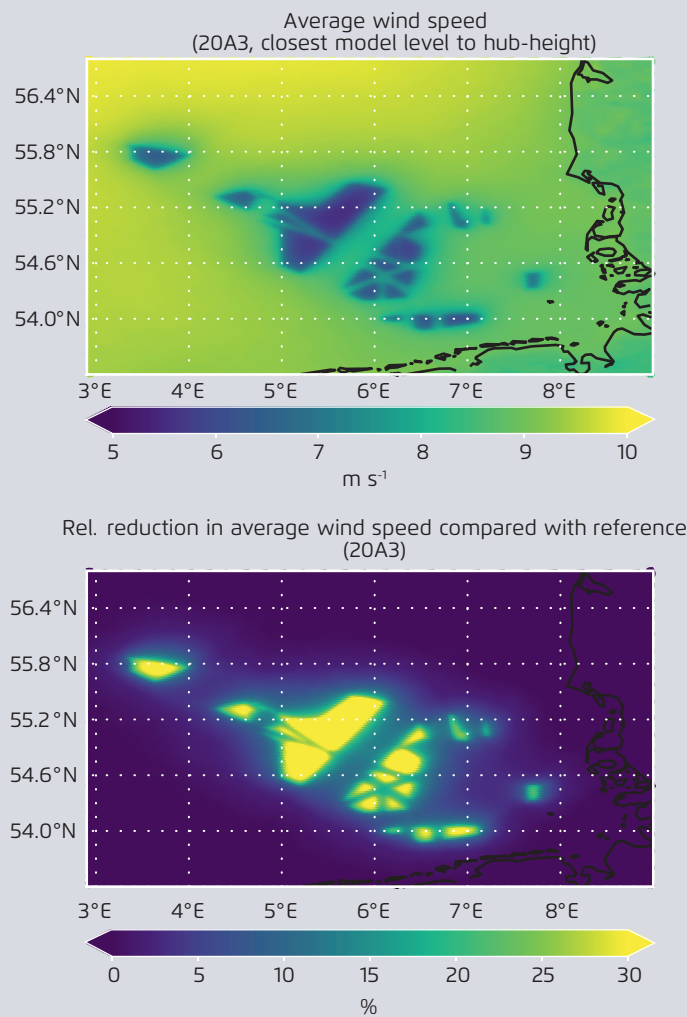
Figure 16



An example where the winds are from the southwest. The colour scale gives the wind speed difference in m/s. The lower wind speeds in the wind farms and surrounding areas mainly downwind of the wind farms and wind farm clusters, can be seen. Higher winds than those in the reference simulation can also be seen.

Maps showing the mean velocity (top) and relative difference of wind speed relative to the reference (bottom) at approximately hub height for scenario 20A3 during the entire simulation period for 2006

Figure 17



DTU (2020)

Windfarm production under different scenarios

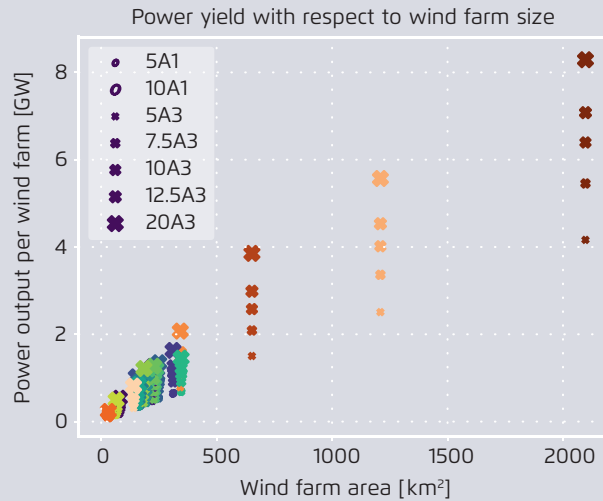
In this section we investigate the power yield of the wind farms indicated in Figure 10 under the different scenarios with mesoscale modelling. The scenarios selected for the mesoscale simulations are given in Table 5.

Figure 18 shows the annual (2006) mean power output for each wind farm and for each of the mesoscale modelled scenarios, plotted against wind farm

area. To understand the plot one can first examine the mean power output of the largest wind farm (SG6), with an area of 2,097.3 km². In the 20A3 scenario the wind farm has a mean power output of 8.3 GW from its nearly 3,495 12 MW turbines. In the scenarios 12.5A3, 10A3, 7.5A3, and 5A3 the mean power output drops to 7.1 GW (from 2,184 turbines), 6.5 GW (from 1,747 turbines), 5.5 GW (from 1,310 turbines), and 4.2 GW (from 873 turbines), respectively. Hence it can be seen that quadrupling the installed capacity

Mean wind farm power output against wind farms area in different scenarios

Figure 18



The colours represent the wind farm in accordance to Figure 10. The scenario is indicated by the symbol and symbol size as indicated by the legend on the top left. Larger wind farms generate more, but the effect is not directly proportional, i.e. a doubled area does not double generation. Similarly, larger installed capacity densities for a given wind farm generate more power.

DTU (2020)

density does not quadruple the mean power output; instead the factor is closer to 2 rather than 4.

Looking at one of the smaller and more isolated wind farms tells a different story. If one looks at the wind farm N4 with an area of 151.9 km², under scenario

20A3, its mean power output is 1.0 GW (from 253 turbines) and under scenario 5A3 it is 0.34 GW (from 63 turbines). Thus the quadrupling of capacity leads to a power output increase of a factor of 3.1.

Table showing the scenarios and scenario notation investigated with the mesoscale modelling

Table 5

| Scenario | Capacity density (MW/km ²) | Area used |
|----------|--|-----------|
| 5A1 | 5.0 | A1 |
| 5A3 | 5.0 | A1 + A2 |
| 7.5A3 | 7.5 | A1 + A2 |
| 10A1 | 10.0 | A1 |
| 10A3 | 10.0 | A1 + A2 |
| 12.5A3 | 12.5 | A1 + A2 |
| 20A3 | 20.0 | A1 + A2 |

DTU (2020)

A similarly sized wind farm in a more crowded setting tells another story again. If one looks at the wind at the wind farm N10 with an area of 161.6 km² in the 20A3 scenario its mean power output is 0.85 GW (from 269 turbines) and in scenario 5A3 it is 0.34 GW (from 67 turbines). Hence, the quadrupling of capacity leads to a power output increase of a factor of 2.5. Although the wind farm is relatively small, its output is behaving more like a very large wind farm, because of its proximity to other wind farms.

Another way to look at Figure 18 is to look at 3 wind farms in the middle range of size (between 310 and 350 km²) in particular N11 (the 4th largest), SG3 (the 5th largest), and N3 (the 6th largest). Their mean power totals in scenario 20A3 differ. The 4th (N11) largest wind farm has a power output over 2 GW, followed by the 6th largest (N3) with 1.7 GW and the 5th largest (SG3) with 1.5 GW.

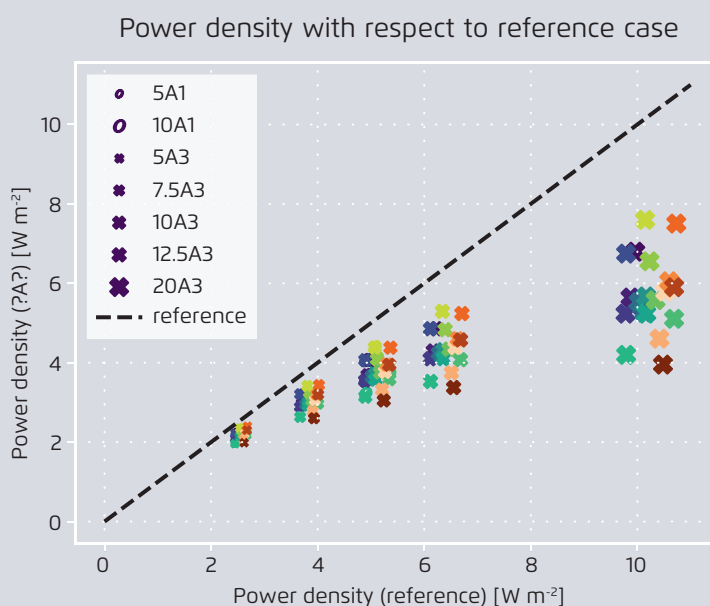
In all of the cases, the reasons for the difference may be explained by (i) the wind farm location having a favourable wind climate, (ii) the wind farm being influenced by its own wakes, (iii) the wind farm being influenced by the wakes of neighbouring wind farms, or a combination of (i), (ii) and (iii).

To determine more precisely the cause of this behaviour, we examined the modelled generated wind farm power density as a function of the nominal reference power density.

For each wind farm, the modelled generated power density is the mean power output (the value used for y-axis of Figure 18) divided by the area of the wind farm (the value used for the x-axis of Figure 18). For each wind farm the nominal reference power density is the hypothetical power the wind farm would produce if there were no wake effects. Any variation in power is due to the wind speed distribution alone. Wind farm modelled generated power density as a

Modelled generated power density compared with nominal reference (no wake) power density in the different scenarios

Figure 19



DTU (2020)

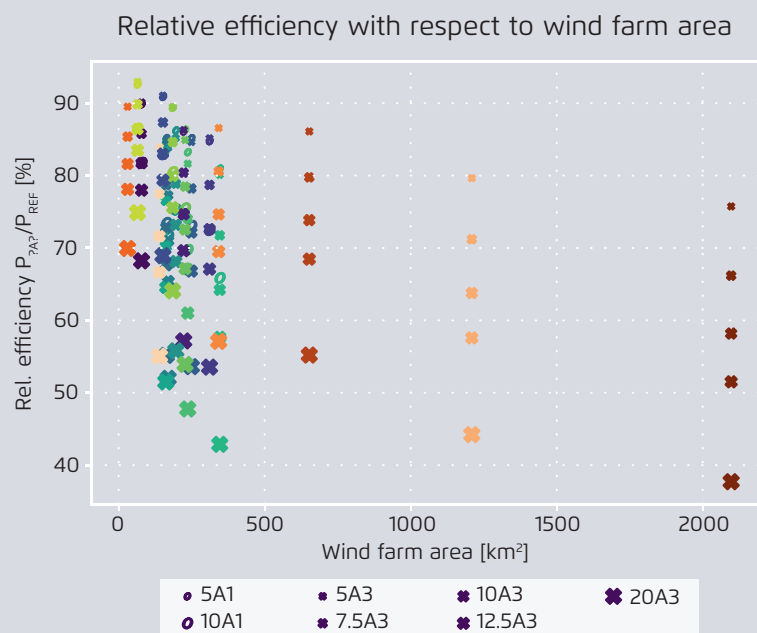
function of the nominal reference power density is shown in Figure 19. First, we examine the largest wind farm (SG6) for the 5A3 scenario, with a nominal reference power density of 2.5 W/m^2 and a modelled generated power density of 2 W/m^2 . The reason these two values are not the same is because of wake effects, both from within the farm and from neighbouring wind farms. The point thus lies under the 1:1 line in the graph. While increasing the installed capacity density increases the nominal reference power density proportionally, the modelled generated power density increases yet reduces the ratio of proportionality, departing further and further from the 1:1 line. This indicates the increasing impact of the wakes on power loss as capacity density rises. The same behaviour is seen in the other wind farms too, but to lesser and varying degrees. The relatively small and isolated wind farm N52 exhibits this effect the least of all.

The ratio of modelled generated wind farm power density to nominal reference power density is the wind farm efficiency. In Figure 20, wind farm efficiency is shown for each wind farm relative to its area. It can be seen here that efficiency is not a function of wind farm size alone. As previously noted, the impact of large neighbouring wind farms is an additional influencing element. Consider wind farm SG4. It has an efficiency of 90 % for scenario 5A3 and 70 % for scenario 20A3. Though this is the smallest wind farm it also has close and very large neighbouring wind farms, and therefore is not the most efficient wind farm. The second smallest wind farm N52 has a higher efficiency, ranging from 92 % for scenario 5A3 to 75 % for scenario 20A3.

Similarly, the wind farm SG5 with its relative isolation performs relatively well compared with the similarly sized N11, which has close and large neighbouring wind farms. The lowest efficiencies are exhibited by the biggest wind farm SG6, where the

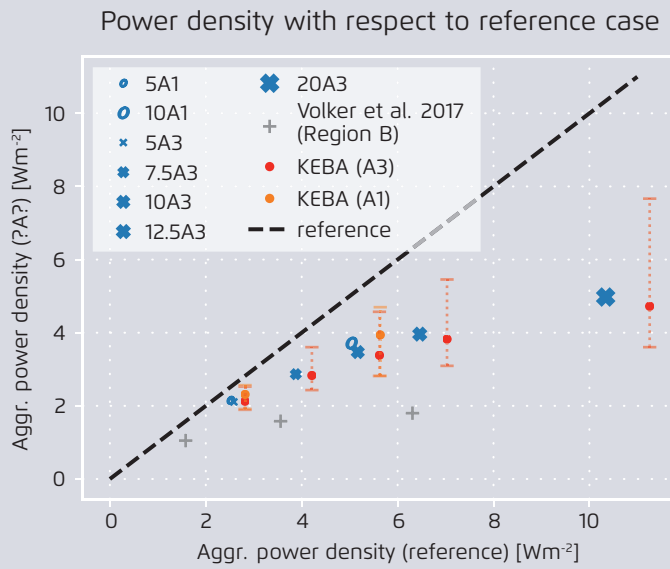
Wind farm efficiency relative to wind farm area in different scenarios

Figure 20



Aggregated generated power density relative to reference power density (no wake) in different scenarios

Figure 21

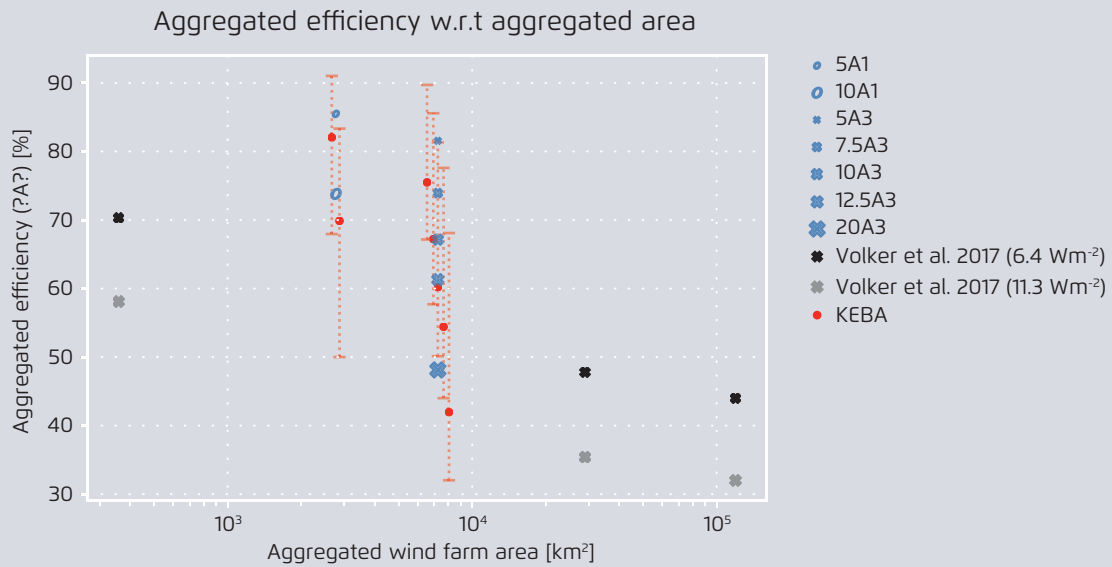


Results from the KEBA method are plotted on the same axis.

DTU (2020)

Aggregated relative efficiency relative to total wind farm area in different scenarios

Figure 22

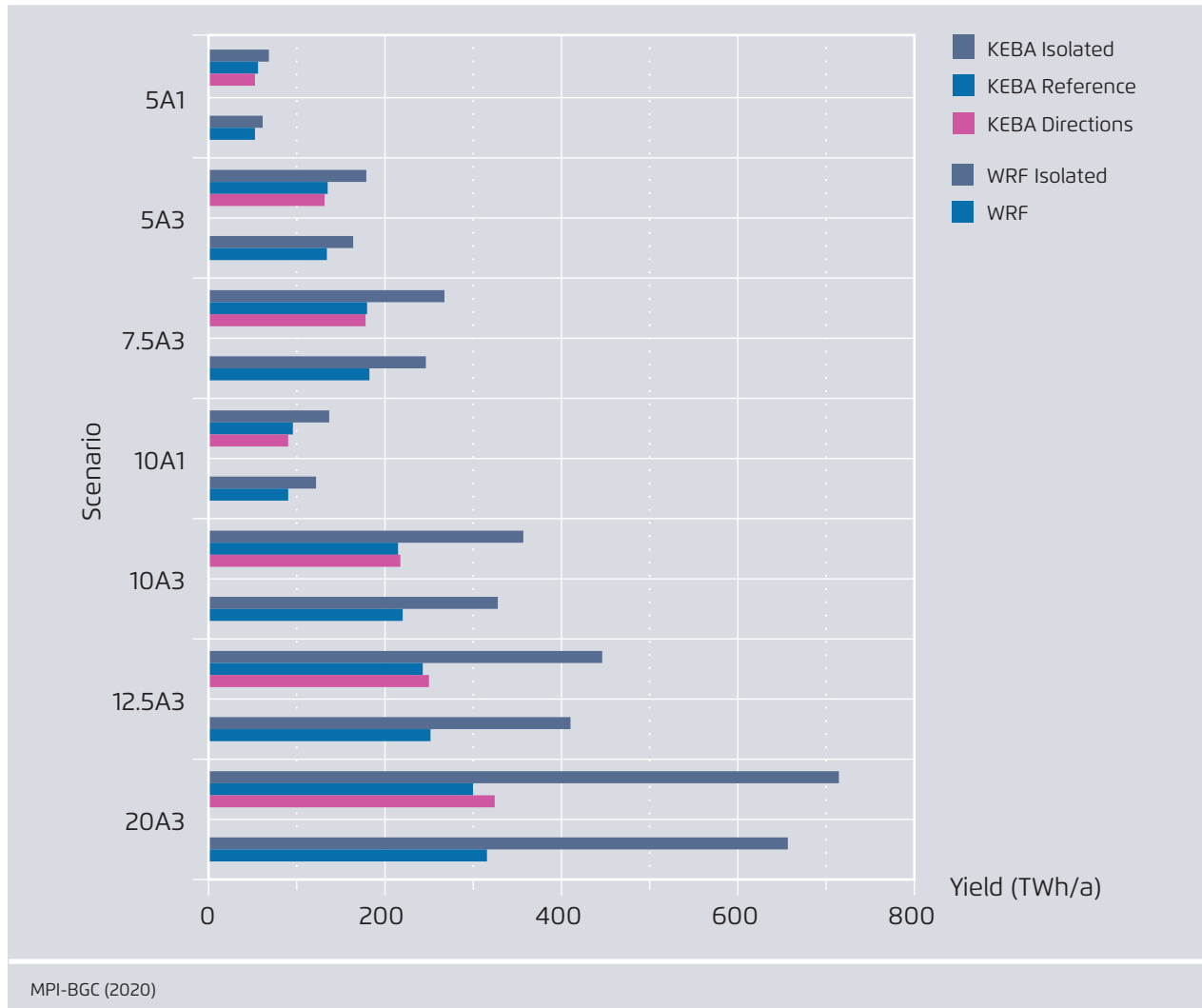


Results from Volker et al. (2017) and from the KEBA method are plotted on the same axis.

DTU (2020)

Comparison of yield estimates between the WRF and KEBA methods
("Reference" and "Directions" cases)

Figure 23



efficiency ranges from 76 % for scenario 5A3 to 38 % for scenario 20A3.

Aggregated results

In this subsection figures from the individual wind farms (Figure 19 and Figure 20) are presented for aggregated wind farm production in each scenario. This provides a very compact overview of the results, though it does not examine individual wind farm performance.

5.4 Comparison and interpretation

Comparison

The estimated yields of both methods are compared in Table 5 and Figures 23 and 24. Both methods show a high level of agreement in terms of yield reduction.

The estimates we used do not account for wake effects or kinetic energy removal ("Isolated" in Figures 23 and 24). The yield estimates differ slightly between the two methods, with the WRF estimate generally about 10 % lower than the KEBA method.

This is attributable to two differences in the forcing. First, WRF uses a single year (2006) for forcing, while KEBA uses observations over the period 2004 – 2015. Second, WRF uses a resolved spatial field with higher wind speeds farther away from the coast (Area 2) than nearer the coast (Area 1). Hence, the full-load hours in scenarios that consider both areas (Area 3) have more full-load hours than the scenarios that only consider Area 1. By contrast, KEBA uses the observations at a single point of the Fino-1 observation station, which may not be representative of the wind fields over Areas 1 and 2.

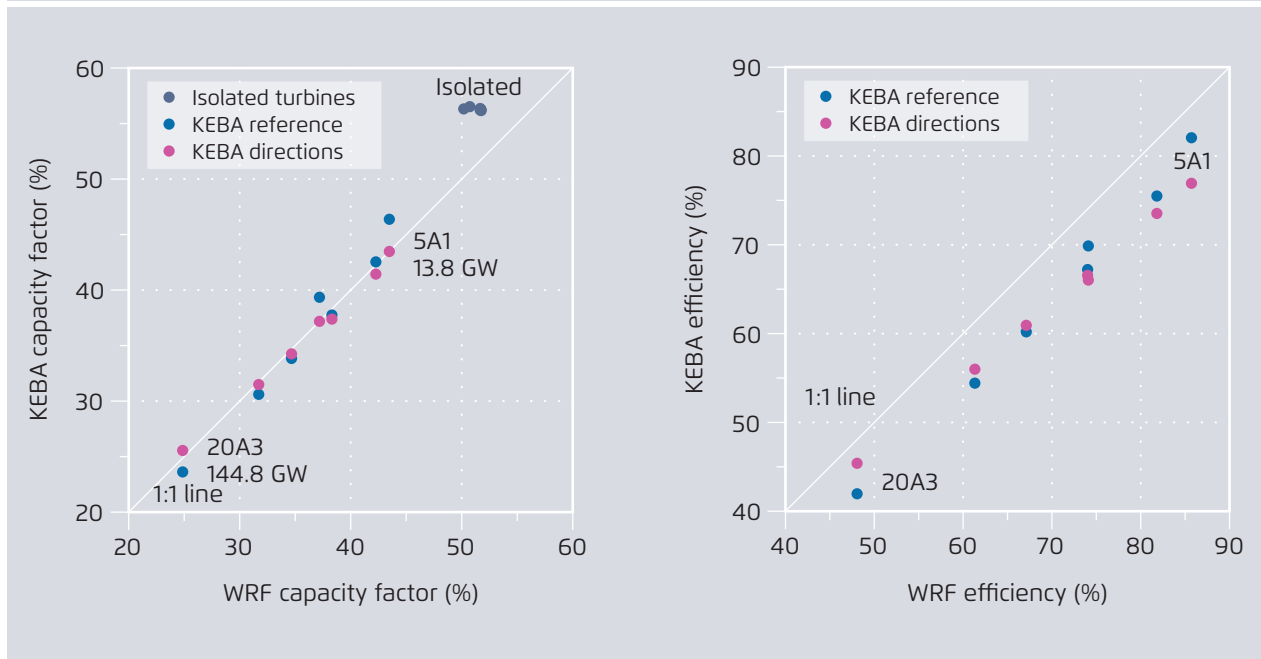
Both methods show a growing yield reduction effect as installed capacities increase (Figure 23), ranging from a comparatively small reduction in the 5A1 scenario to a large reduction by more than 50% in the 20A3 scenario. This reduction is reflected in the average capacity factors, which decline from more than 50% in the “Isolated” reference estimates to about 25% in the 20A3 scenario (Figure 24), reducing

the full-load hours from 4,528 to 4,928 hours per year down to 2,070 to 2,179 hours per year.

The yield reductions associated with installed capacity increases are more easily seen by considering the effect on the average efficiency of the turbine (Figure 24). Turbine efficiency compares the yield estimate that accounts for the wind speed reduction to the yield without this reduction. An efficiency of 100% represents the yield of an isolated, single turbine that sees no effects of wind speed reduction. In the scenario with the lowest installed capacity (5A1), WRF estimates a reduction of the efficiency to 85%, while KEBA estimates a reduction of the efficiency to 82%, representing a difference of 4% between the methods. For the scenarios with the highest installed capacity (20A3), WRF estimates a reduction of the efficiency to 48%, while KEBA estimates a reduction of the efficiency to 42%, representing a difference of 13%.

Comparison of WRF estimates with KEBA estimates (“Reference” and “Directions” cases) for capacity factors and efficiencies

Figure 24



MPI-BGC (2020)

While discrepancies in the estimates exist, they are relatively minor compared with the overall yield reduction in the “Isolated” cases. It should be noted, however, that neither approach takes into account other potential causes for inefficiencies that could further lower yields.

Interpretation

Both methods show a remarkable level of agreement regarding the overall magnitude of yield reductions caused by wind turbines. While the WRF method uses a state-of-the-art weather forecasting simulation model, the KEBA method uses a budget approach to measure the flows of kinetic energy into the wind farm regions. But both models capture the reduction effects on wind speeds that are caused by the removal of kinetic energy from the turbines. And both show that large-scale deployments of wind turbines in the North Sea region are likely to lower yields in the region.

The reason for the yield reductions can be understood by the atmospheric flows of kinetic energy (Figure 15). The scenarios with greater installed capacities approach levels that are similar to the levels of kinetic energy that the atmosphere supplies to the wind farm region. As these yield reduction effects relate to the atmosphere, technological advances in the turbines are unlikely to be able to offset them, although one may be able to minimize the detrimental effects through better planning of wind farm layouts in the region.

These yield reductions appear to be significant in magnitude and would therefore need to be considered in reasonable estimates about what to expect from offshore wind energy in scenarios for the year 2050.

Full results from the KEBA and WRF simulations

| Formulation of scenarios | | | | | | Results | | | | | | |
|---|----------------|-------------|-------------------------------|--------------------------|------------------|------------|------|---------------------|-------|--------------------------|------|--------------------------------|
| Density (W/m ² or MW/km ²) | Included areas | | Installed capacity (GW) | Number of turbines | Scenario name | No wake | | | | | | |
| | Area 1 | Area 2 | | | | Yield (GW) | | Full-load hours [h] | | Capacity factor (CF) [%] | | CF difference KEBA - WRF |
| | 2767 km2 | 4473 km2 | | | | WRF | KEBA | WRF | KEBA | WRF | KEBA | |
| | | | | | | | | | | | | |
| 5 | x | | 13.8 | 1,153 | 5A1 | 7.0 | 7.8 | 4,410 | 4,928 | 50 % | 56 % | 12 % |
| 5 | | x | 22.4 | 1,864 | 5A2 | | 12.6 | | 4,928 | | 56 % | |
| 5 | x | x | 36.2 | 3,017 | 5A3 | 18.7 | 20.4 | 4,528 | 4,928 | 52 % | 56 % | 9 % |
| 7.5 | x | | 20.8 | 1,730 | 7.5A1 | | 11.7 | | 4,928 | | 56 % | |
| 7.5 | | x | 33.5 | 2,796 | 7.5A2 | | 18.9 | | 4,928 | | 56 % | |
| 7.5 | x | x | 54.3 | 4,525 | 7.5A3 | 28.1 | 30.5 | 4,528 | 4,928 | 52 % | 56 % | 9 % |
| 10 | x | | 27.7 | 2,306 | 10A1 | 13.9 | 15.6 | 4,410 | 4,928 | 50 % | 56 % | 12 % |
| 10 | | x | 44.7 | 3,728 | 10A2 | | 25.2 | | 4,928 | | 56 % | |
| 10 | x | x | 72.4 | 6,033 | 10A3 | 37.4 | 40.7 | 4,528 | 4,928 | 52 % | 56 % | 9 % |
| 12.5 | x | | 34.6 | 2,883 | 12.5A1 | | 19.5 | | 4,928 | | 56 % | |
| 12.5 | | x | 55.9 | 4,660 | 12.5A2 | | 31.5 | | 4,928 | | 56 % | |
| 12.5 | x | x | 90.5 | 7,541 | 12.5A3 | 46.8 | 50.9 | 4,538 | 4,928 | 52 % | 56 % | 9 % |
| 20 | x | | 55.3 | 4,612 | 20A1 | | 31.1 | | 4,928 | | 56 % | |
| 20 | | x | 89.5 | 7,455 | 20A2 | | 50.3 | | 4,928 | | 56 % | |
| 20 | x | x | 144.8 | 12,067 | 20A3 | 74.9 | 81.5 | 4,528 | 4,928 | 52 % | 56 % | 9 % |

DTU and MPI-BGC (2020)

Table 6

| Results | | | | | | | | | |
|---|------|---------------------|-------|----------------------|------|-----------------------------|---------------|------|-----------------------------------|
| With wakes caused by kinetic energy removal | | | | | | | | | |
| Yield (GW) | | Full-load hours [h] | | Capacity factor* [%] | | CF difference KEBA - WRF | Efficiency[%] | | Efficiency difference KEBA-WRF |
| WRF | KEBA | WRF | KEBA | WRF | KEBA | | WRF | KEBA | |
| 6.0 | 6.4 | 3,770 | 4,065 | 43% | 46% | -8% | 85% | 82% | -4% |
| | 10.0 | | 3,913 | | 45% | | | 79% | |
| 15.3 | 15.4 | 3,693 | 3,729 | 42% | 43% | -1% | 82% | 75% | -8% |
| | 8.8 | | 3,713 | | 42% | | | 75% | |
| | 13.5 | | 3,530 | | 40% | | | 71% | |
| 20.8 | 20.5 | 3,348 | 3,309 | 38% | 38% | 1% | 74% | 67% | -9% |
| 10.3 | 10.9 | 3,255 | 3,449 | 37% | 39% | -6% | 74% | 70% | -6% |
| | 16.4 | | 3,216 | | 37% | | | 65% | |
| 25.1 | 24.5 | 3,040 | 2,966 | 35% | 34% | 2% | 67% | 60% | -10% |
| | 12.6 | | 3,190 | | 36% | | | 65% | |
| | 18.8 | | 2,949 | | 34% | | | 60% | |
| 28.7 | 27.7 | 2,776 | 2,683 | 32% | 31% | 3% | 61% | 54% | -11% |
| | 16.4 | | 2,600 | | 30% | | | 53% | |
| | 23.8 | | 2,331 | | 27% | | | 47% | |
| 36.0 | 34.2 | 2,179 | 2,070 | 25% | 24% | 5% | 48% | 42% | -13% |

* Other losses not included

6 Conclusions

We evaluated different scenarios for offshore wind energy in the German Bight of the North Sea ranging from 13.8 to 144.8 GW of installed capacity. This covers the range in published scenarios of offshore wind energy in 2050 for the German energy transition. We investigated the extent to which the scenario yields are lowered by reduced wind speeds due to the effects of wind turbines, which extract kinetic energy from the atmospheric flow. We used two approaches to evaluate these scenarios: the KEBA approach, a simple accounting of the kinetic energy budget; and the WRF approach, a highly detailed numerical simulation of the atmosphere.

Both approaches predict similar levels of yield reductions due to the effects of wind speeds across the range of scenarios. These reductions are more moderate – 82–85 % of the yield from an isolated turbine – in the case of the scenario with the lowest installed capacity (13.8 GW). The reductions rise as installed capacity increases. By the high scenario (144.8 GW), reductions amount to 42 – 48 % of the yield from an isolated turbine.

The agreement between the two methods is quite remarkable and suggests that it is the supply of kinetic energy from atmospheric flows not the technical specifications of the wind turbines that is the primary limitation at these scales. This is further supported by a previous study,²⁰ which considered different turbine technology but found similar yield reduction levels.

From these results we conclude that **wind speed reductions need to be considered in German energy scenarios for offshore wind energy** in view of the fact that they substantially lower expected yields.

20 Volker et al. (2017)

7 Recommendations

This study suggests that in order to make better use of offshore wind energy, **wind farms should be planned and developed with a coordinated long-term approach** that considers the co-dependency of installed capacity density and areal coverage for efficient deployment.

Based on our conclusion and potential shortcomings of our study, we also recommend further research ranging from the validation of yield reductions as wind farms expand in scale to potential implications for cross-country effects and onshore wind energy.

Evaluation of limitations and validation. Limitations of the approach include a limited validation of meso-scale modelling windfarm wake parameterizations, especially with regard to turbine size, the horizontal extent of wind farm clusters and installed capacity densities. We recommend that research projects be undertaken to validate the models used in this study. Such projects will require collaboration between the wind energy industry and research institutes in order to understand the complicated datasets associated with the operations of the multiple windfarms and the atmospheric processes that need to be modelled. It is recommended that some kind of trusted sharing of wind farm production data would be used when validating our methods.

Comparison with engineering wake models. Another valuable study would be the assessment of the extent to which current practices, mainly via the use of engineering models to determine wake losses fail to account for the efficiency reductions estimated in this study. The engineering models sufficiently capture intra-windfarm and inter-windfarm wake losses only when the horizontal extent of the wind-farm areas is relatively small. At what horizontal extents and installed capacity densities does the feedback to large-scale flows become a significant part of the wind farm impact on the environment, and

therefore essential to include in an energy resource calculation? It is important to evaluate this question and derive new recommendations on how planners and the wind industry can better estimate resources while accounting for the larger scale impacts of wind farm wakes.

Onshore effects. As offshore wind farms extract kinetic energy and cause substantial areas of depleted wind speeds in the downwind direction, one may ask about whether and how far these effects extend to coastal areas. This question is important to assess, as reduced wind speeds could lower the yields of coastal onshore wind energy.

Cross-border effects. In this study, we considered reasonable, large-scale deployment of wind turbines in the German Bight, but we did not consider offshore wind farm developments in neighbouring regions, such as the Netherlands, the United Kingdom, or Denmark. Such developments in upwind areas could cause regions of depleted wind speeds that extend to the German Bight, potentially reducing the wind energy yields of offshore wind energy in the German section of the North Sea. Our results suggest that it is mainly the horizontal flow of kinetic energy that sustains a high wind energy potential in the offshore region. The impact of this flow due to windfarm development upwind poses an important scientific problem to be evaluated. It also indicates that scenarios for the development of offshore wind energy should be performed across national borders to make efficient use of offshore wind energy.

8 References

- acatech et al. (2017):** "Sektorkopplung" – Untersuchungen und Überlegungen zur Entwicklung eines integrierten Energiesystems. Analyse.
- Agora Energiewende (2020):** *Die Energiewende im Stromsektor: Stand der Dinge 2019. Rückblick auf die wesentlichen Entwicklungen sowie Ausblick auf 2020.* https://www.agora-energiewende.de/fileadmin2/Projekte/2019/Jahresauswertung_2019/171_A-EW_Jahresauswertung_2019_WEB.pdf
- Badger, J. and Volker, P.J. (2017):** *Efficient large-scale wind turbine deployment can meet global electricity generation needs.* Proceedings of the National Academy of Sciences, 114(43), pp. E8945–E8945.
- BDI (2018):** *Klimapfade für Deutschland.* BCG, Prognos, commissioned by Bundesverband der Deutschen Industrie (BDI)
- BMU (2015):** *Klimaschutzszenario 2050.* 2. Endbericht, Öko-Institut, Fh-ISI, commissioned by Bundesministerium für Umwelt (BMU).
- C3S (Copernicus Climate Change Service) (2017):** *ERA5: Fifth generation of ECMWF atmospheric reanalyses of the global climate.* Copernicus Climate Change Service Climate Data Store (CDS), <https://cds.climate.copernicus.eu/cdsapp#!/home>
- Corten, G. (2001):** *Novel Views on the Extraction of Energy from Wind-Heat Generation Concentration and Terrain,* EWEC-CONFERENCE 2001.
- Deutsche WindGuard (2018):** *Status of Offshore Wind Energy Development in Germany. Year 2018.* Commissioned by BWE, BWO, Stiftung Offshore Windenergie, VDMA Power Systems and wab. https://www.wind-energie.de/fileadmin/redaktion/dokumente/dokumente-englisch/publications/Factsheet__Status_of_Offshore_Wind_Energy_Development_in_Germany_Year_2018.pdf
- Donlon, C.J., Martin, M., Stark, J., Roberts-Jones, J., Fiedler, E. and Wimmer, W. (2012):** *The operational sea surface temperature and sea ice analysis (OSTIA) system.* *Remote Sensing of Environment*, 116, pp. 140–158.
- Fitch, A.C., Olson, J.B., Lundquist, J.K., Dudhia, J., Gupta, A.K., Michalakes, J. and Barstad, I. (2012):** *Local and mesoscale impacts of wind farms as parameterized in a mesoscale NWP model.* *Monthly Weather Review*, 140(9), pp. 3017–3038.
- Gans, F., Miller, L. M., Kleidon, A. (2012):** *The problem of the second wind turbine – a note on a common but flawed wind power estimation method.* *Earth System Dynamics*, 3, pp. 79–86.
- Gustavson, M. R. (1979):** *Limits to wind power utilization,* *Science*, 204, pp. 13–17.
- Kleidon, A. (2010):** *Life, hierarchy, and the thermodynamic machinery of planet Earth,* *Phys. Life Rev.*, 7, pp. 424–460.
- Langor, E.N. (2019):** *Characteristics of Offshore Wind Farm Wakes and their Impact on Wind Power Production from Long-term Modelling and Measurements,* DTU Wind Energy-M-0315, Master of Science Dissertation.

Lorenz, E. (1955): *Available potential energy and the maintenance of the general circulation*, *Tellus*, 7, pp. 271–281.

Lundquist, J.K., DuVivier, K.K., Kaffine, D. and Tomaszewski, J.M. (2019): *Costs and consequences of wind turbine wake effects arising from uncoordinated wind energy development*. *Nature Energy*, 4(1), p.26.

Miller, L. M., Gans, F., and Kleidon, A. (2011): *Estimating maximum global land surface wind power extractability and associated climatic consequences*, *Earth Syst. Dynam.*, 2, pp. 1–12, doi:10.5194/esd-2-1-2011.

Miller, L. M., Kleidon, A. (2016): *Wind speed reductions by large-scale wind turbine deployments lower turbine efficiencies and set low generation limits*. *Proc. Natl. Acad. Sci. USA*, 113(48), pp. 13570–13575. doi:10.1073/pnas.1602253113

MWV (2018): *Status und Perspektiven flüssiger Energieträger in der Energiewende*. Prognos AG, Fh-UMSICHT, DBFZ, commissioned by Mineralölwirtschaftsverband e.V. (MWV), IWO, MEW, UNITI

Skamarock, W.C., Klemp, J.B., Dudhia, J., Gill, D.O., Barker, D.M., Wang, W. and Powers, J.G. (2008): *A description of the Advanced Research WRF version 3*. NCAR Technical note-475+ STR.

Stiftung Offshore (2017): *Energiewirtschaftliche Bedeutung der Offshore-Windenergie für die Energiewende*. Update 2017, Fh-IWES, commissioned by Stiftung Offshore Windenergie.

Volker, P. J. H., Hahmann, A. N., Badger, J., and Jørgensen, H. E. (2017): *Prospects for generating electricity by large onshore and offshore wind farms*. *Environmental Research Letters* 12 (2017) 034022. doi: 10.1088/1748-9326/aa5d86

Volker, P.H.J., Badger, J., Hahmann, A.N. and Ott, S. (2015): *The Explicit Wake Parametrisation V1.0: a wind farm parametrisation in the mesoscale model WRF*. *Geoscientific Model Development Discussions*, 8, pp. 3481–3522.

9 Appendices

9.1 Parameter values used for the KEBA method

Total yield P_{el} and an effective wind speed v within the wind farm region are estimated in KEBA using the kinetic energy budget of the air volume that encloses the wind farm region (Kleidon and Miller, in preparation). This budgeting results in a reduction factor, f_{red} , which is given by

$$f_{red} = \frac{H+2C_d L}{H+2C_d L + \frac{3N\eta A_{rotor}}{2 W}}$$

for the case in which the turbines operate below their capacity. From this reduction factor, the effective wind speed v and the total yield P_{el} are estimated by

$$v = f_{red}^{1/3} v_{in}$$

$$P_{el} = f_{red} \frac{\rho}{2} \eta N A_{rotor} v_{in}^3$$

The parameters used to evaluate the KEBA method are as follows:

| | |
|-----------------------------------|--------------------------------------|
| Air density | $\rho = 1.2 \text{ kg m}^{-3}$ |
| Turbine efficiency | $\eta = 0.42$ |
| Rotor area | $A_{rotor} = 31416 \text{ m}^2$ |
| Turbine capacity | $P_{max} = 12 \times 10^6 \text{ W}$ |
| Cut-in velocity | $v_{in} = 3 \text{ ms}^{-1}$ |
| Cut-out velocity | $v_{out} = 28 \text{ ms}^{-1}$ |
| Height of maritime boundary layer | $H = 700 \text{ m}$ |
| Drag coefficient | $C_d = 0.001$ |

Number of turbines N , cross-sectional width W , and downwind length L were specified depending on the scenario used.

9.2 Cross-sectional widths and downwind lengths used in the KEBA "directions" estimates

For the KEBA "directions" estimate, the FINO-1 time series is separated into histograms for the eight different main wind directions (North, North-East, East, South-East, South, South-West, West, North-West). For each of the wind directions, a separate KEBA estimate is performed and afterwards combined to yield the total estimate. For the different wind directions, different values for cross-sectional width and downwind lengths are used, as shown in Figures 25 and 26 and specified in Table 7.

Note that for different wind directions and areas used a different number of clusters exists. For instance, for the NW wind direction using Area 3, all clusters are aligned along the downwind direction, so that this configuration is treated as one cluster in KEBA. For the SW wind direction, the areas with wind farms appear as four separate clusters, yielding different dimensions for the KEBA estimate.

Cross-sectional widths W and downwind lengths L for the different clusters depicted in Figures 25 and 26.

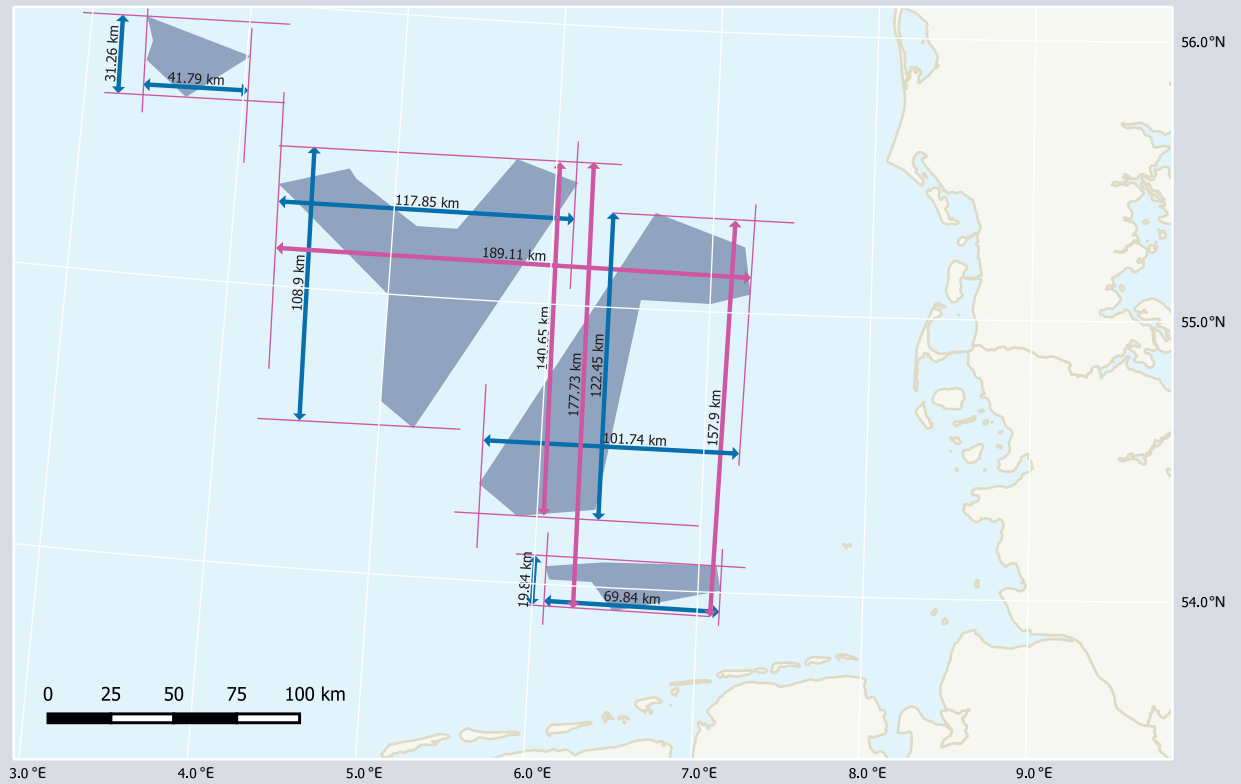
Table 7

| Area 1 | | | | | |
|-----------------------|---------------------------|---------------------|----------------------|---------------------|----------------------|
| Wind direction | Number of clusters | Width 1 (km) | Length 1 (km) | Width 2 (km) | Length 2 (km) |
| N and S | 1 | 101.7 | 157.9 | - | - |
| NE and SW | 2 | 72.2 | 142.8 | 53.7 | 53.3 |
| E and W | 2 | 122.5 | 101.7 | 19.8 | 69.8 |
| SE and NW | 1 | 145.6 | 128.8 | - | - |
| Area 2 | | | | | |
| N and S | 2 | 117.9 | 108.9 | 41.8 | 31.3 |
| NE and SW | 2 | 108.7 | 117.0 | 39.0 | 32.6 |
| E and W | 2 | 108.9 | 117.9 | 31.3 | 41.8 |
| SE and NW | 1 | 117.0 | 192.5 | - | - |
| Area 3 | | | | | |
| N and S | 2 | 189.1 | 177.7 | 41.8 | 31.3 |
| NE and SW | 4 | 39.0 | 32.6 | 108.7 | 117.0 |
| E and W | 3 | 31.3 | 41.8 | 177.7 | 189.1 |
| SE and NW | 1 | 148.0 | 321.3 | - | - |
| | | Width 3 (km) | Length 3 (km) | Width 4 (km) | Length 4 (km) |
| N and S | | - | - | - | - |
| NE and SW | | 72.2 | 142.8 | 53.7 | 53.3 |
| E and W | | 19.8 | 69.8 | - | - |
| SE and NW | | - | - | - | - |

MPI-BGC (2020)

Dimensions of cross-sectional widths and downwind lengths used in the KEBA "directions" estimates for the wind directions N, E, S, and W

Figure 25



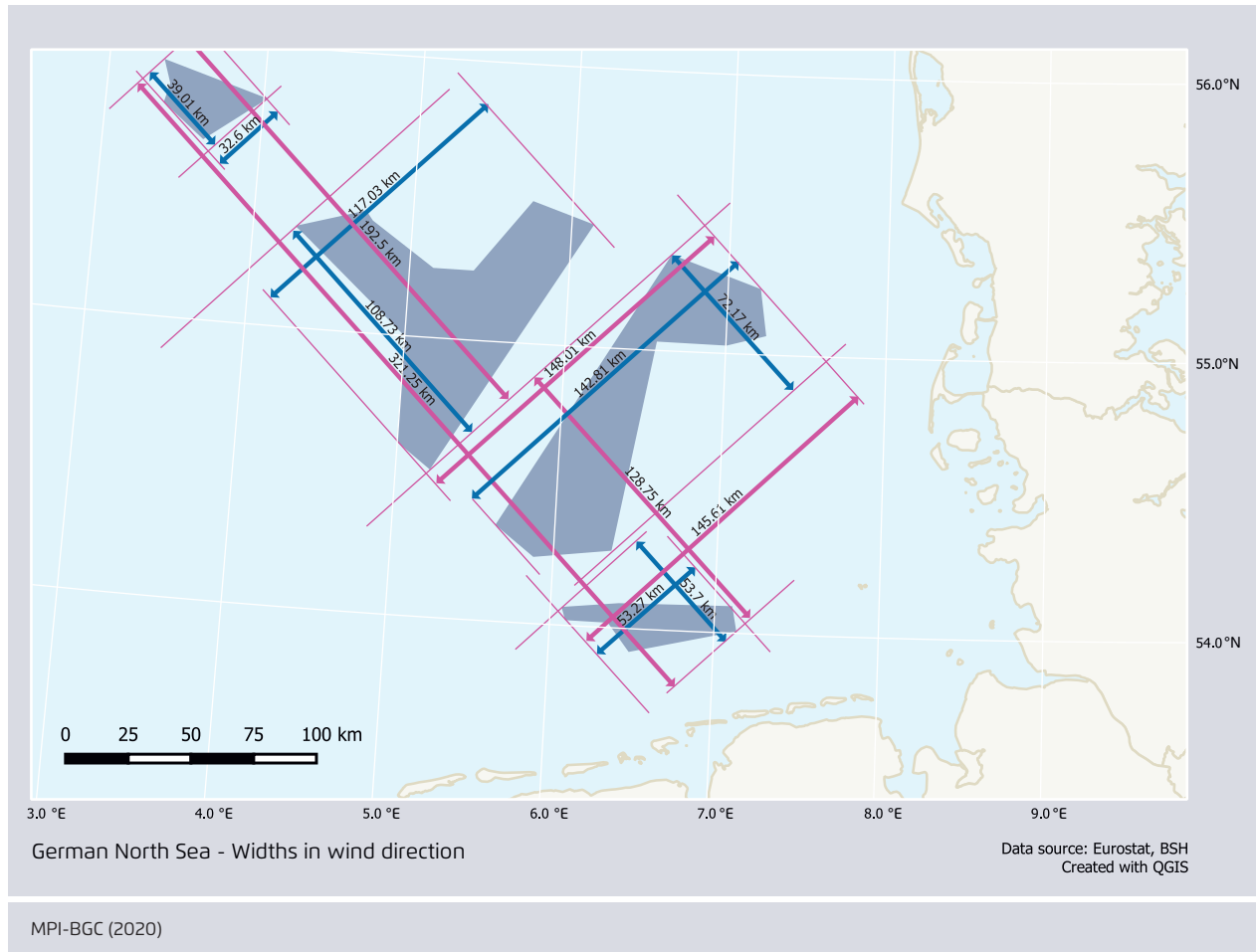
German North Sea - Widths in W-E and N-S direction

Data source: Eurostat, BSH
Created with QGIS

MPI-BGC (2020)

Dimensions of cross-sectional widths and downwind lengths used in the KEBA "directions" estimates for the wind directions NW, NE, SW, and SE

Figure 26



9.3 Namelist for the WRF mesoscale model

```

&time_control
start_year          = YY1, YY1, YY1
start_month         = MM1, MM1, MM1
start_day           = DD1, DD1, DD1
start_hour          = HH1, HH1, HH1
start_minute        = 00, 00, 00
start_second        = 00, 00, 00
end_year            = YY2, YY2, YY2
end_month           = MM2, MM2, MM2
end_day             = DD2, DD2, DD2
end_hour            = HH2, HH2, HH2
end_minute          = 00, 00, 00
end_second          = 00, 00, 00
interval_seconds    = 21600,
input_from_file     = .T., .T., .T.
history_interval    = 240, 120, 60
frames_per_outfile  = 6, 12, 24
restart             = .false.
restart_interval    = 100000
io_form_history     = 2
io_form_restart     = 2
io_form_input       = 2
io_form_boundary    = 2
iofields_filename   = „WAFieldsNew.txt“,
                    „WAFieldsNew.txt“,
                    „WAFieldsNew.txt“
auxinput4_inname    = „wrfinp_d<domain>“
auxinput4_interval  = 360,360,360
io_form_auxinput4   = 2
ignore_iofields_warning = .true.
debug_level         = 0
/

&domains
max_dom             = 3,
time_step           = 90,
use_adaptive_time_step = .true.
step_to_output_time = .true.
target_cfl          = 1.2, 1.2, 1.2
target_hcfl         = 0.84, 0.84, 0.84
max_step_increase_pct = 51, 51, 51

starting_time_step  = 90, 30, 5
max_time_step       = 100, 36, 12
min_time_step       = 16, 4, 2
adaptation_domain   = 1,
parent_id            = 0, 1, 2
parent_grid_ratio    = 1, 3, 3
j_parent_start       = 1, 21, 45
i_parent_start       = 1, 50, 80
s_sn                 = 1, 1, 1
s_we                 = 1, 1, 1
e_we                 = 166, 247, 310
e_sn                 = 101, 169, 262
e_vert               = 61, 61, 61
grid_id              = 1, 2, 3
parent_time_step_ratio = 1, 3, 3
num_metgrid_levels   = 33
num_metgrid_soil_levels = 4
dx                   = 18000.,6000.,2000.
dy                   = 18000.,6000.,2000.
p_top_requested      = 5000,
eta_levels           = 1.000000, 0.998600, 0.996000,
                    0.994000, 0.992000, 0.990000,
                    0.987592, 0.984486, 0.980977,
                    0.977016, 0.972544, 0.967500,
                    0.961813, 0.955403, 0.948185,
                    0.940062, 0.930929, 0.920670,
                    0.909158, 0.896257, 0.881820,
                    0.859633, 0.830162, 0.794019,
                    0.751945, 0.704330, 0.659043,
                    0.615990, 0.575078, 0.536219,
                    0.499329, 0.464324, 0.431126,
                    0.399657, 0.369845, 0.341616,
                    0.314904, 0.289641, 0.265763,
                    0.243210, 0.221922, 0.201841,
                    0.182641, 0.164410, 0.148206,
                    0.132526, 0.117709, 0.104002,
                    0.091398, 0.079808, 0.069150,
                    0.059351, 0.050340, 0.042054,
                    0.034434, 0.027428, 0.020986,
                    0.015062, 0.009615, 0.004606,
                    0.000000
smooth_option        = 2,
feedback             = 0,
/

```

```

max_step_increase_pct = 5, 51, 51
starting_time_step = 90, 30, 10
max_time_step = 135, 45, 12
min_time_step = 27, 9, 3

max_step_increase_pct = 51, 51, 51
starting_time_step = 90, 30, 5
max_time_step = 100, 36, 12
min_time_step = 16, 4, 2

j_parent_start = 1, 20, 40
i_parent_start = 1, 40, 93

e_we = 158, 277, 340
e_sn = 101, 169, 262

starting_time_step = 90, 30, 10

min_time_step = 27, 9, 3

&physics
mp_physics = 4, 4, 4
ra_lw_physics = 4, 4, 4
ra_sw_physics = 4, 4, 4
swint_opt = 1
radt = 10, 10, 10
sf_surface_physics = 2, 2, 2
sf_sfclay_physics = 5, 5, 5
bl_pbl_physics = 5, 5, 5
cu_physics = 1, 0, 0
cudt = 5, 5, 5
isfflx = 1,
icloud = 1,
surface_input_source = 1,
num_land_cat = 28,
num_soil_layers = 4,
sst_update = 1,
windfarm_opt = 0, 0, 2
windfarm_ij = 0,
windturbines_spec = „windturbines.real“
ROfrac = 1.5,
/

&fdda
grid_fdda = 2, 0, 0
gfdda_inname = "wrrfdda_d<domain>",
gfdda_end_h = 300, 0, 0
gfdda_interval_m = 360, 0, 0
fgdt = 0, 0, 0
if_no_pbl_nudging_uv = 0, 0, 0
if_no_pbl_nudging_t = 1, 0, 0
if_no_pbl_nudging_q = 1, 0, 0
if_zfac_uv = 1, 0, 0
k_zfac_uv = 20, 0, 0
if_zfac_t = 1, 0, 0
k_zfac_t = 20, 0, 0
if_zfac_q = 1, 0, 0
k_zfac_q = 20, 0, 0
guv = 0.0003, 0.000075,
0.000075
gt = 0.0003, 0.000075,
0.000075
gq = 0003, 0.000075,
0.000075
xwavenum = 14
ywavenum = 10
if_ramping = 0
dtramp_min = 60.0
io_form_gfdda = 2
/

&dynamics
w_damping = 1
diff_opt = 1
km_opt = 4
diff_6th_opt = 2, 2, 2
diff_6th_factor = 0.06, 0.08, 0.1
damp_opt = 0
zdamp = 5000., 5000., 5000.
dampcoef = 0.15, 0.15, 0.15
khdif = 0, 0, 0
kvdif = 0, 0, 0
non_hydrostatic = .true.,.true.,.true.
moist_adv_opt = 1, 1, 1
scalar_adv_opt = 1, 1, 1
/

```

```
base_temp          = 290.

&bdy_control
spec_bdy_width    = 5
spec_zone         = 1
relax_zone        = 4
specified         = .true., .false., .false.
nested           = .false., .true., .true.
/

&grib2
/

&namelist_quilt
nio_tasks_per_group = 0,
nio_groups          = 1,
/
```

Publications by Agora Energiewende

IN ENGLISH

Supporting the Energy Transition in the Western Balkans

The German Power Market: State of Affairs in 2019

State of Affairs in 2019

The Liberalisation of Electricity Markets in Germany

History, Development and Current Status

A Word on Low Cost Renewables

The Renewables Breakthrough: How to Secure Low Cost Renewables

Building sector Efficiency: A crucial Component of the Energy Transition

Final report on a study conducted by Institut für Energie- und Umweltforschung Heidelberg (Ifeu), Fraunhofer IEE and Consentec

Climate-neutral industry (Executive Summary)

Key technologies and policy options for steel, chemicals and cement

Distribution grid planning for a successful energy transition – focus on electromobility

Conclusions of a study commissioned by Agora Verkehrswende, Agora Energiewende and Regulatory Assistance Project (RAP)

Unlocking Low Cost Renewables in South East Europe

Case Studies on De-risking Onshore Wind Investment

Climate (Un)ambition in South East Europe

A Critical Assessment of the Draft National Energy and Climate Plans

The German Coal Commission

A Roadmap for a Just Transition from Coal to Renewables

The Southeast European power system in 2030

Flexibility challenges and regional cooperation benefits

The French CO₂ Pricing Policy:

Learning from the Yellow Vests Protests

European Energy Transition 2030: The Big Picture

Ten Priorities for the next European Commission to meet the EU's 2030 targets and accelerate towards 2050

All publications are available on our website: www.agora-energiewende.de

Publications by Agora Verkehrswende

IN ENGLISH

En route to Paris?

Implications of the Paris Agreement for the German transport sector

Distribution grid planning for a successful energy transition – focus on electromobility

Conclusions of a study commissioned by Agora Verkehrswende, Agora Energiewende and Regulatory Assistance Project (RAP)

Shared E-Scooters: Paving the Road Ahead

Policy Recommendations for Local Government

New Roads to Sustainable Travel

Communication Strategies for Behaviour Change

Towards Decarbonising Transport | 2018

A 2018 Stocktake on Sectoral Ambition in the G20

Supporting a U-Turn in Parking Policy

Facts and Figures

The new EU regulation on CO2 emissions from cars and how it impacts carbon targets in Germany's transport sector

The Future Cost of Electricity-Based Synthetic Fuels

Ensuring a Sustainable Supply of Raw Materials for Electric Vehicles

A Synthesis Paper on Raw Material Needs for Batteries and Fuel Cells

Transforming Transport to Ensure Tomorrow's Mobility

12 Insights into the Verkehrswende

All publications are available on our website: www.agora-verkehrswende.de

How do we accomplish the clean-energy transition? Which legislation, initiatives and measures do we need to make it a success? Agora Energiewende and Agora Verkehrswende are helping Germany set the course towards a fully decarbonised energy system. As think-&-do-tanks, we work with key stakeholders to enhance the knowledge base and facilitate a convergence of views.



This publication is available for
download under this QR code.

Agora Energiewende

Anna-Louisa-Karsch-Strasse 2 | 10178 Berlin, Germany
P +49 (0)30 700 14 35-000
F +49 (0)30 700 14 35-129
www.agora-energiewende.de
info@agora-energiewende.de

Agora Verkehrswende

Anna-Louisa-Karsch-Strasse 2 | 10178 Berlin, Germany
P +49 (0)30 700 14 35-000
F +49 (0)30 700 14 35-129
www.agora-verkehrswende.de
info@agora-verkehrswende.de

